

The solution of the A_r T-system for arbitrary boundary

Philippe Di Francesco

Department of Mathematics, University of Michigan,
530 Church Street, Ann Arbor, MI 48190, USA
and Institut de Physique Théorique du Commissariat à l'Énergie Atomique,
Unité de recherche associée du CNRS, CEA Saclay/IPhT/Bat 774,
F-91191 Gif sur Yvette Cedex, France

`philippe.di-francesco@cea.fr`

Submitted: Feb 23, 2010; Accepted: Jun 3, 2010; Published: Jun 14, 2010

Mathematics Subject Classification: 05C88

Abstract

We present an explicit solution of the A_r T -system for arbitrary boundary conditions. For each boundary, this is done by constructing a network, i.e. a graph with positively weighted edges, and the solution is expressed as the partition function for a family of non-intersecting paths on the network. This proves in particular the positive Laurent property, namely that the solutions are all Laurent polynomials of the initial data with non-negative integer coefficients.

1 Introduction

In this paper we study the solutions of the A_r T -system, namely the following coupled system of recursion relations for $\alpha, j, k \in \mathbb{Z}$:

$$T_{\alpha,j,k+1}T_{\alpha,j,k-1} = T_{\alpha,j+1,k}T_{\alpha,j-1,k} + T_{\alpha+1,j,k}T_{\alpha-1,j,k} \quad (1.1)$$

for $\alpha \in I_r = \{1, 2, \dots, r\}$, and subject to the boundary conditions

$$T_{0,j,k} = T_{r+1,j,k} = 1 \quad (j, k \in \mathbb{Z}) \quad (1.2)$$

This system arose in many different contexts. The system (1.1) and its generalizations were introduced as the set of relations satisfied by the eigenvalues of the fused transfer matrices of generalized quantum spin chains based on any simply-laced Lie algebra \mathfrak{g} [2] [16]; in this paper we restrict ourselves to the case $\mathfrak{g} = sl_{r+1}$, but we believe our constructions can be adapted to other \mathfrak{g} 's as well.

With the additional condition that $T_{\alpha,0,k} = 1$, $k \in \mathbb{Z}$ and the restriction to $j \in \mathbb{Z}_+$, the solutions of (1.1-1.2) were also interpreted as the q -characters of some representations of the affine Lie algebra $U_q(\widehat{sl}_{r+1})$, the so-called Kirillov-Reshetikhin modules [12], indexed by $\alpha \in I_r = \{1, 2, \dots, r\}$ and $j \in \mathbb{Z}_+$, while k stands for a discrete spectral parameter [18].

The same equations appeared in the context of enumeration of domino tilings of plane domains [21], and was studied in its own right under the name of octahedron equation [15] [14]. As noted by many authors, this equation may also be viewed as a particular case of Plücker relations when all T 's are expressed as determinants involving only the $T_{1,j,k}$'s. These particular Plücker relations are also known as the Desnanot-Jacobi relation, used by Dodgson to devise his famous algorithm for the computation of determinants [9]. In [20], this equation was slightly deformed by introducing a parameter λ before the second term on the r.h.s. and used to define the "lambda-determinant", with a remarkable expansion on alternating sign matrices, generalizing the usual determinant expansion over permutations. Here we will not consider such a deformation, although we believe our constructions can be adapted to include this case as well (see [21] for a general discussion, which however does not cover the A_r case).

Viewing the system (1.1) as a three-term recursion relation in $k \in \mathbb{Z}$, it is clear that the solution is entirely determined in terms of some initial data that covers two consecutive values of k , say $k = 0, 1$ and say all $j \in \mathbb{Z}$. In [7], an explicit expression for $T_{\alpha,j,k}$ was derived as a function of the initial data $\mathbf{x}_0 = \{T_{\alpha,j,0}, T_{\alpha,j,1}\}_{\alpha \in I_r, j \in \mathbb{Z}}$. It involved expressing first $T_{1,j,k}$ as the partition function for weighted paths on some particular target graph, with weights that are monomials of the initial data, and then interpreting $T_{\alpha,j,k}$ as the partition of non-intersecting families of such paths. This interpretation was then extended to other initial data of the form

$$\mathbf{x}_{\mathbf{k}} = \{T_{\alpha,j,k_\alpha}, T_{\alpha,j,k_\alpha+1}\}_{\alpha \in I_r, j \in \mathbb{Z}} \quad (1.3)$$

where $\mathbf{k} = (k_1, k_2, \dots, k_r) \in \mathbb{Z}^r$ is a Motzkin path of length $r - 1$, namely $k_{\alpha+1} - k_\alpha \in \{0, 1, -1\}$ for all $\alpha = 1, 2, \dots, r - 1$. In this construction, for each Motzkin path \mathbf{k} , the expressions for the $T_{\alpha,j,k}$ in terms of the initial data $\mathbf{x}_{\mathbf{k}}$ are also partition functions of weighted paths on some target graph $\Gamma_{\mathbf{k}}$.

The equation (1.1) is also connected to cluster algebras. In Ref. [4], it was shown that the initial data sets $\mathbf{x}_{\mathbf{k}}$ form a particular subset of clusters in a suitably defined cluster algebra. Roughly speaking, a cluster algebra [11] is a dynamical system expressing the evolution of some initial data set (cluster), with the built-in property that any evolved data is expressible as Laurent polynomials of any other data set. This Laurent property or Laurent phenomenon turned out to be even more powerful than expected, as all the known examples show that these polynomials have *non-negative integer* coefficients. The positivity conjecture of [11] states that this property holds in general. As an example, the above-mentioned lambda-determinant relation may be viewed as an evolution equation in the same cluster algebra as in [4], with λ as a coefficient: the existence of an expansion formula of the lambda-determinant on alternating sign matrices is a manifestation of the positive Laurent phenomenon. As another example, the explicit expressions of [7] for the solutions $T_{\alpha,j,k}$ of the A_r T -system as partition functions for positively weighted paths

gives a direct proof of Laurent positivity for the relevant clusters.

However, the set of initial data $\mathbf{x}_{\mathbf{k}}$ (1.3) covered in [7] is limited to sets of $T_{\alpha,j,k}$'s with fixed values of $k = k_{\alpha}$ independently of j . The most general set of initial data should also allow for inhomogeneities in j , namely values of $k = k_{\alpha,j}$ varying with j as well. It is easy to see that the most general boundary condition consists in assigning fixed positive values $(a_{\alpha,j})_{\alpha \in I_r; j \in \mathbb{Z}}$ to $T_{\alpha,j,k_{\alpha,j}}$ along a “stepped surface” (also called solid-on-solid interface in the physics literature), namely such that $|k_{\alpha+1,j} - k_{\alpha,j}| = 1$ and $|k_{\alpha,j+1} - k_{\alpha,j}| = 1$ for all $\alpha \in I_r$ and $j \in \mathbb{Z}$.

In this paper we address the most general case of initial data for the A_r T -system (1.1-1.2). As we will show, initial data are in bijection with configurations of the six-vertex model with face labels on a strip of square lattice of height $r - 1$ and infinite width. For any such given set of initial data, we derive an explicit expression for the solution $T_{\alpha,j,k}$ (1.1-1.2) as the partition function for α non-intersecting paths on a suitable network, in the spirit of Refs. [10] and [19], and with step weights that are Laurent monomials of the initial data. This completes the proof of the Laurent positivity of the solutions of the A_r T -system for arbitrary initial data.

The paper is organized as follows.

Our construction was originally inspired by Ref.[1] which basically deals with the case of A_1 under the name of “friezes”¹: the latter is reviewed in Section 2, where we make in particular the connection between the frieze language and the solutions of the A_1 T -system with arbitrary boundary data. Roughly speaking, the solution is expressed as the element of a matrix product taken along the boundary.

A warmup generalization to the case of A_2 is presented in Section 3, with the main Theorem 3.4 giving an explicit solution for arbitrary boundary data, also as an element of a matrix product taken along the boundary.

Section 4 is devoted to the general A_r case. Starting from the path solution of [7] for some particular initial data, we construct various transfer matrices associated to the boundary, with simple transformations under local elementary changes of the boundary (mutations). For convenience, boundaries are expressed as configurations of the six-vertex model in an infinite strip of finite height $r - 1$. These in turn encode a network, entirely determined by the boundary data. The final result is an explicit formula Theorem 4.12 for the solution of the A_r T -system as the partition function for families of non-intersecting paths.

In Section 5, we study the restrictions of our results to the Q -system.

A few concluding remarks are gathered in Section 6.

¹Strictly speaking the term frieze only refers to the particular cases of integer-valued boundary conditions, for which the entire solution is integer-valued. Here, we use this term in a broader sense, including arbitrary boundary conditions as well, and would correspond more to what is called “ SL_2 -tilings of the plane” in Ref.[1].

2 A_1 T -system and Frises

In this section, we first review the results of [1], and then rephrase them in terms of solutions to the A_1 T -system for arbitrary boundary conditions.

2.1 Friezes

2.1.1 Frieze equation

The frieze equation reads²:

$$u_{a+1,b-1}u_{a,b} = 1 + u_{a+1,b}u_{a,b-1} \quad (2.1)$$

for $a, b \in \mathbb{Z}$.

2.1.2 Boundaries

The most general (infinite) boundary condition is along a “staircase”, made of horizontal (h) and vertical (v) steps of the form $h : (x, y) \rightarrow (x + 1, y)$ and $v : (x, y) \rightarrow (x, y + 1)$, giving rise to a sequence of vertices (x_j, y_j) , $j \in \mathbb{Z}$. To each vertex of the sequence we attach a positive number a_j , $j \in \mathbb{Z}$, and the boundary condition for the system (2.1) reads:

$$u_{x_j, y_j} = a_j \quad (j \in \mathbb{Z}) \quad (2.2)$$

The simplest such boundary is the sequence $\dots hvhvhv\dots$, say with variable a_{2x} at vertex (x, x) and a_{2x+1} at vertex $(x, x + 1)$, $x \in \mathbb{Z}$. We refer to it as the *basic staircase boundary*.

The problem is now to find the solution $u_{a,b}$ of (2.1) with the boundary condition (2.2).

2.1.3 Projection of (x, y) on the boundary and step matrices

The general solution at a point (x, y) to the right of the boundary is expressed solely in terms of the values (2.2) taken by u along the “projection” of (x, y) onto the boundary, defined as follows.

Definition 2.1 (Projection). *The projection of (x, y) onto the boundary $\{(x_j, y_j)\}_{j \in \mathbb{Z}}$ is the sequence (x_j, y_j) , $j = t, t + 1, \dots, t'$, where $y_t = y$, $x_{t'} = x$, and the first step $t \rightarrow t + 1$ is vertical, while the last step $t' - 1 \rightarrow t'$ is horizontal.*

This is illustrated in Fig.2.1. Alternatively the projection of (x, y) is coded by the word $w(x, y) = v\dots h$ of length $t' - t$ with letters h and v, starting with v and ending with h and coding the succession of horizontal (h) and vertical (v) steps along the boundary between (x_t, y_t) and $(x_{t'}, y_{t'})$. We also define the corresponding sequence of boundary weights $\mathbf{a}(x, y) = (a_t, a_{t+1}, \dots, a_{t'})$.

²Our convention corresponds to $b \rightarrow -b$ in those of Ref [1].

Example 2.5 (The basic staircase boundary). For any $x > y \in \mathbb{Z}_{\geq 0}$, we have a projection on the boundary with $w(x, y) = (vh)^{x-y}$, and $\mathbf{a}(x, y) = (a_{2y}, a_{2y+1}, \dots, a_{2x})$. We deduce that

$$M(w(x, y), \mathbf{a}(x, y)) = \prod_{i=y}^{x-1} V(a_{2i}, a_{2i+1})H(a_{2i+1}, a_{2i+2}) \quad (2.6)$$

and the solution reads:

$$u_{x,y} = a_{2x} (M(w(x, y), \mathbf{a}(x, y)))_{1,1} \quad (2.7)$$

Explicitly, we compute the two-step matrix:

$$M(a, b, c) = V(a, b)H(b, c) = \frac{1}{c} \begin{pmatrix} \frac{ac+1}{b} & 1 \\ 1 & b \end{pmatrix} \quad (2.8)$$

2.1.5 Mutations

Note that we may move from one boundary to another by elementary “mutations”³, namely the local substitution $(v, h) \rightarrow (h, v)$ on the boundary (forward mutation) or $(h, v) \rightarrow (v, h)$ (backward mutation), while the sequence \mathbf{a} is updated using the frieze relation (2.1). In particular, we may in principle reach any boundary from the basic staircase one, by possibly infinitely many such mutations.

The effect of such a mutation is easily obtained by computing the corresponding matrix transformation within $M(w, \mathbf{a})$. It basically corresponds to the following identity:

Lemma 2.6. For all $a, b, c > 0$, we have:

$$V(a, b)H(b, c) = H(a, x)V(x, c), \quad x = \frac{1 + ac}{b} \quad (2.9)$$

This may be understood as a matrix representation of the mutation via the commutation of the matrices V and H , which acquire the new boundary value x in replacement for b . This mutation affects all values of $u_{m,p}$ such that the projection of (m, p) contains the new boundary point with value x .

We may deduce the general formula (2.5) from that for the basic staircase boundary, by induction under mutation. In general a mutation simply switches two consecutive matrices $VH \rightarrow HV$ in the product M . We must be careful with mutations that update the extremal vertices of the projection of (x, y) , namely in the two cases: (i) when w starts with vh , updated into hv or (ii) when w ends up with vh , updated into hv . We note however that $H(a, b)_{1,j} = bV(a, b)_{j,1} = \delta_{i,j}$ hence in the updated matrix M we may: (i) drop the first matrix factor H (ii) drop the last matrix factor V , but replace the scalar prefactor by the new updated vertex value, and the formula (2.5) follows.

³The term “mutation” is borrowed from cluster algebras, as this elementary move indeed corresponds to a mutation in the associated cluster algebra of [7].

2.2 The A_1 T-system

2.2.1 T-system

The A_1 T-system reads:

$$T_{j,k+1}T_{j,k-1} = T_{j+1,k}T_{j-1,k} + 1 \quad (2.10)$$

where we use the shorthand notation $T_{j,k} = T_{1,j,k}$ for $j, k \in \mathbb{Z}$. Note that this splits into two independent systems for fixed value of $j + k$ modulo 2.

In the case when $j + k = 0$ modulo 2, we immediately see that changing to “light cone” coordinates: $a = \frac{j+k}{2}$ and $b = \frac{j-k}{2}$, we have that $u_{a,b} = T_{j,k-1}$ satisfies the frieze equation (2.1). So the two problems are equivalent. Analogously, when $j + k = 1$ modulo 2, we take $a = \frac{j+k-1}{2}$ and $b = \frac{j-k+1}{2}$ and $u_{a,b} = T_{j,k}$.

2.2.2 Boundaries

The fundamental boundary for the T-system is obtained by fixing the values of say $T_{2j+1,0}$ and $T_{2j,1}$ for all $j \in \mathbb{Z}$. It corresponds to the basic staircase boundary in the case $j + k = 1$ modulo 2 above, with $T_{2j,1} = a_{2j}$ and $T_{2j+1,0} = a_{2j+1}$.

Other boundaries are mapped in an obvious manner.

2.2.3 Path solution

In [7], an explicit path formulation was derived for the solution $T_{j,k}$ for the fundamental boundary condition. Defining the 4×4 transfer matrix

$$\mathcal{T}(u, v, w) = \begin{pmatrix} 0 & 1 & 0 & 0 \\ u & 0 & 1 & 0 \\ 0 & v & 0 & 1 \\ 0 & 0 & w & 0 \end{pmatrix}$$

we have

Theorem 2.7 ([7]). *The solution of the A_1 T-system (2.10) for the fundamental boundary condition with initial data $\{T_{2j+1,0}, T_{2j,1}\}_{j \in \mathbb{Z}}$ reads for $j + k = 1 \pmod 2$:*

$$\begin{aligned} T_{j,k} &= T_{j+k,0} \left(\prod_{i=j-k}^{j+k-1} \mathcal{T}(u_i, v_i, w_i) \right)_{1,1} \\ u_i &= \frac{T_{i,1}}{T_{i+1,0}}, \quad v_i = \frac{1}{T_{i,0}T_{i+1,1}}, \quad w_i = \frac{1}{u_i} \end{aligned} \quad (2.11)$$

Here the matrix $\mathcal{T}(i, i + 1) \equiv \mathcal{T}(u_i, v_i, w_i)$ is interpreted as the transfer matrix from time i to time $i + 1$ for weighted paths with steps $a \rightarrow a \pm 1$ on the integer segment $[0, 3]$, with time-dependent step weights $0 \rightarrow 1 : u_i$, $1 \rightarrow 2 : v_i$ and $2 \rightarrow 3 : w_i$, the other weights being equal to 1.

2.2.4 Gauge invariance

The above formula (2.11) remains clearly unchanged if we transform the matrix \mathcal{T} into the following: $\mathcal{T}(i, i+1) \rightarrow \tilde{\mathcal{T}}(i, i+1) = L_i \mathcal{T}(i, i+1) L_{i+1}^{-1}$, for any invertible matrix L_i such that $(L_i)_{1,j} = \delta_{j,1}$ and $(L_i)_{j,1} = \delta_{j,1}$.

To make the contact with the frieze solution, let us define $\tilde{\mathcal{T}}$ as above, by use of the matrix

$$L_i = \begin{pmatrix} 1 & 0 & 0 & 0 \\ 0 & 1 & 0 & 0 \\ 0 & 0 & T_{i,0} & 0 \\ 0 & 0 & 0 & T_{i,1} \end{pmatrix}$$

2.2.5 Comparison with the frieze solution

Let us now compute the “two-step” transfer matrix at times $i, i+1$ for $i = j+k$ modulo 2: $\tilde{\mathcal{T}}(i, i+2) = \tilde{\mathcal{T}}(i, i+1) \tilde{\mathcal{T}}(i+1, i+2)$, with the weights as in (2.11), namely:

$$\begin{aligned} u_i &= \frac{b_i}{b_{i+1}}, & v_i &= \frac{1}{a_i a_{i+1}}, & w_i &= \frac{1}{u_i} \\ u_{i+1} &= \frac{a_{i+1}}{a_{i+2}}, & v_{i+1} &= \frac{1}{b_{i+1} b_{i+2}}, & w_{i+1} &= \frac{1}{u_{i+1}} \end{aligned}$$

where we have introduced $a_i = T_{i,0}$, $a_{i+1} = T_{i+1,1}$, $a_{i+2} = T_{i+2,0}$, $b_i = T_{i,1}$, $b_{i+1} = T_{i+1,0}$, and $b_{i+2} = T_{i+2,1}$, while $L_i = \text{diag}(1, 1, a_i, b_i)$, $L_{i+1} = \text{diag}(1, 1, b_{i+1}, a_{i+1})$ and $L_{i+2} = \text{diag}(1, 1, a_{i+2}, b_{i+2})$.

We get:

$$\tilde{\mathcal{T}}(i, i+2) = \begin{pmatrix} \frac{a_{i+1}}{a_{i+2}} & 0 & \frac{1}{a_{i+2}} & 0 \\ 0 & \frac{1+b_i b_{i+2}}{b_{i+1} b_{i+2}} & 0 & \frac{1}{b_{i+2}} \\ \frac{1}{a_{i+2}} & 0 & \frac{1+a_i a_{i+2}}{a_{i+1} a_{i+2}} & 0 \\ 0 & \frac{1}{b_{i+2}} & 0 & \frac{b_{i+1}}{b_{i+2}} \end{pmatrix}$$

This 4×4 matrix clearly decomposes into two independent 2×2 linear operators acting respectively on components 1, 3 and 2, 4. The corresponding matrices are respectively:

$$\begin{aligned} \tilde{\mathcal{P}}(i, i+2) &= \begin{pmatrix} \frac{a_{i+1}}{a_{i+2}} & \frac{1}{a_{i+2}} \\ \frac{1}{a_{i+2}} & \frac{1+a_i a_{i+2}}{a_{i+1} a_{i+2}} \end{pmatrix} = H(a_i, a_{i+1}) V(a_{i+1}, a_{i+2}) \\ \tilde{\mathcal{Q}}(i, i+2) &= \begin{pmatrix} \frac{1+b_i b_{i+2}}{b_{i+1} b_{i+2}} & \frac{1}{b_{i+2}} \\ \frac{1}{b_{i+2}} & \frac{b_{i+1}}{b_{i+2}} \end{pmatrix} = V(b_i, b_{i+1}) H(b_{i+1}, b_{i+2}) \end{aligned}$$

We may now use the gauge-transformed and reduced two-step transfer matrix $\tilde{\mathcal{P}}(i, i+2)$ instead of \mathcal{T} in (2.11). Indeed, in the product over steps from $j-k$ to $j+k-1$, we may pair up consecutive \mathcal{T} matrices in (2.11) to express it in terms of the \mathcal{P} 's, and then substitute the latter with the $\tilde{\mathcal{P}}$'s, leading to:

$$T_{j,k} = T_{j+k,0} \left(\prod_{i=0}^{k-1} \tilde{\mathcal{P}}(j-k+2i, j-k+2i+2) \right)_{1,1}$$

Noting moreover that $H(a, b)_{1,j} = bV(a, b)_{j,1} = \delta_{j,1}$, we may rewrite this as

$$T_{j,k} = T_{j+k-1,1} \left(\prod_{i=0}^{k-2} V(a_{j-k+2i+1}, a_{j-k+2i+2}) H(a_{j-k+2i+2}, a_{j-k+2i+3}) \right)_{1,1} \quad (2.12)$$

Assuming that $j + k = 1$ modulo 2, we see that in light-cone coordinates with $x = \frac{j+k-1}{2}$ and $y = \frac{j-k+1}{2}$, equation (2.12) amounts to equations (2.6-2.7), as the projection of (x, y) on the boundary staircase starts at $t = j - k + 1$ and ends at $t' = j + k - 1$.

2.2.6 Mutations and arbitrary boundary

As in the frieze case, this identification gives us access to mutations, via the $VH \leftrightarrow HV$ identity (2.9). Starting from (2.12), we may iteratively apply forward/backward mutations to the basic staircase boundary to get any other boundary (up to global translations) of the form $\{T_{j,k_j}\}_{j \in \mathbb{Z}}$ with a sequence $k_j \in \mathbb{Z}$ such that $|k_{j+1} - k_j| = 1$. Let us denote by (j_0, k_{j_0}) and (j_1, k_{j_1}) the extremities of the projection of (j, k) onto the boundary, namely such that $j_0 - k_{j_0} = j - k$, $j_1 + k_{j_1} = j + k$, j_0 maximal and j_1 minimal.

We deduce that the general solution for arbitrary staircase boundary reads:

$$T_{j,k} = T_{j_1, k_{j_1}} \left(V(T_{j_0, k_{j_0}}, T_{j_0+1, k_{j_0+1}}) \dots H(T_{j_1-1, k_{j_1-1}}, T_{j_1, k_{j_1}}) \right)_{1,1}$$

where the product is taken along the projection of (j, k) on the boundary, with a matrix V per vertical step and H per horizontal step.

3 The A_2 T-system with arbitrary boundary

Before going to the general A_r case, we derive the A_2 solution in detail.

3.1 T-system

The A_2 T-system reads:

$$\begin{aligned} T_{1,j,k+1} T_{1,j,k-1} &= T_{1,j+1,k} T_{1,j-1,k} + T_{2,j,k} \\ T_{2,j,k+1} T_{2,j,k-1} &= T_{2,j+1,k} T_{2,j-1,k} + T_{1,j,k} \end{aligned} \quad (3.1)$$

for $j, k \in \mathbb{Z}$. Note that this splits again into two independent systems for $T_{\alpha,j,k}$ with fixed value of $\alpha + j + k$ modulo 2. These indices run over two consecutive layers of the centered cubic lattice $\alpha = 1$ and $\alpha = 2$, which form two square lattices, the vertices of the second layer lying at the vertical of the centers of the faces of the first layer.

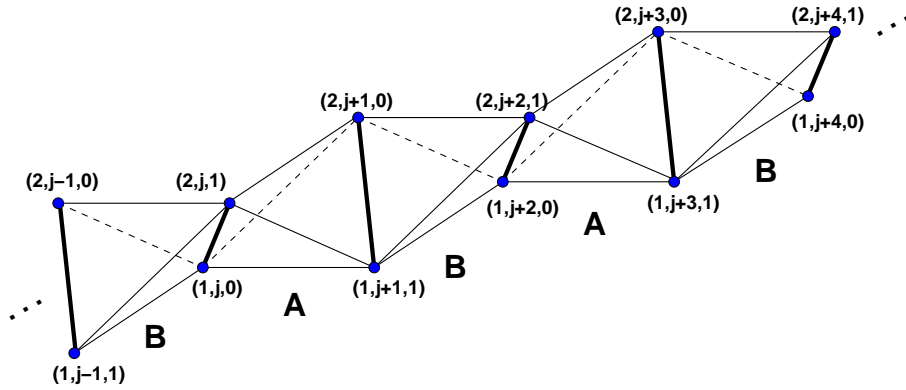


Figure 3.1: The basic staircase boundary for the A_2 T -system. We have indicated the corresponding succession of edges (thick black line) and the two types of tetrahedrons A,B that connect them.

3.2 Boundaries

The fundamental boundary considered in Ref. [7] involves fixing the values of the $T_{\alpha,j,k}$ with $\alpha = 1, 2$ $k = 0, 1$, and $j \in \mathbb{Z}$, with fixed parity of $\alpha + j + k$ (say even). We refer to this boundary as the *basic staircase* boundary, in reference to the A_1 case. It can be viewed as an infinite strip made of a succession of four kinds of vertices (see Fig.3.1). We may also view this strip as a succession of edges of the form $e_j = (1, j, 0) - (2, j, 1)$, $f_{j+1} = (1, j + 1, 1) - (2, j + 1, 0)$, $e_{j+2} = (1, j + 2, 0) - (2, j + 2, 1)$, etc. for $j - 1 \in 2\mathbb{Z}$ (thick black lines in Fig.3.1). Two such consecutive edges define a tetrahedron. The basic staircase may therefore be viewed as the alternating succession of two kinds of tetrahedrons denoted by A (defined by e_j, f_{j+1}) and B (defined by f_{j-1}, e_j).

3.3 Solution for the basic staircase boundary

In Ref. [7], the solution $T_{1,j,k}$ was expressed in terms of paths on a target graph with 6 vertices and with time-dependent edge weights involving only the boundary values. These weights are coded by a 6×6 transfer matrix. Defining:

$$\mathcal{T}(s, t, u, v, w) = \begin{pmatrix} 0 & 1 & 0 & 0 & 0 & 0 \\ s & 0 & 1 & 0 & 0 & 0 \\ 0 & t & 0 & 1 & 1 & 0 \\ 0 & 0 & u & 0 & 0 & 0 \\ 0 & 0 & v & 0 & 0 & 1 \\ 0 & 0 & 0 & 0 & w & 0 \end{pmatrix} \quad (3.2)$$

and using the notation

$$s_i = \frac{T_{1,i,1}}{T_{1,i+1,0}}, \quad t_i = \frac{T_{2,i,1}}{T_{1,i,0}T_{1,i+1,1}}, \quad u_i = \frac{T_{1,i+1,0}T_{2,i-1,1}}{T_{1,i,1}T_{2,i,0}}, \quad v_i = \frac{T_{1,i+1,0}}{T_{2,i,0}T_{2,i+1,1}}, \quad w_i = \frac{T_{2,i+1,0}}{T_{2,i,1}} \quad (3.3)$$

we have:

Theorem 3.1 ([7]). *The solution of the A_2 T -system for $\alpha = 1$ reads:*

$$T_{1,j,k} = T_{1,j+k,0} \left(\prod_{i=j-k}^{j+k-1} \mathcal{T}(s_i, t_i, u_i, v_i, w_i) \right)_{1,1} \quad (3.4)$$

3.4 Reduced transfer matrix

As before we note that the two-step transfer matrix $\mathcal{T}(i, i+2) = \mathcal{T}(i, i+1)\mathcal{T}(i+1, i+2)$, with $\mathcal{T}(i, i+1) \equiv \mathcal{T}(s_i, t_i, u_i, v_i, w_i)$, is again decomposable into two linear operators acting respectively on components (1, 3, 6) and (2, 4, 5). Explicitly:

$$\mathcal{T}(s, t, u, v, w)\mathcal{T}(s', t', u', v', w') = \begin{pmatrix} s' & 0 & 1 & 0 & 0 & 0 \\ 0 & s+t' & 0 & 1 & 1 & 0 \\ ts' & 0 & t+u'+v' & 0 & 0 & 1 \\ 0 & ut' & 0 & u & u & 0 \\ 0 & vt' & 0 & v & v+w' & 0 \\ 0 & 0 & wv' & 0 & 0 & w \end{pmatrix}$$

Defining:

$$\mathcal{P}(i, i+2) = \begin{pmatrix} s_{i+1} & 1 & 0 \\ t_i s_{i+1} & t_i + u_{i+1} + v_{i+1} & 1 \\ 0 & w_i v_{i+1} & w_i \end{pmatrix}$$

we may rewrite (3.4) as:

$$T_{1,j,k} = T_{1,j+k,0} \left(\prod_{i=0}^{k-1} \mathcal{P}(j-k+2i, j-k+2i+2) \right)_{1,1} \quad (3.5)$$

3.5 Gauge transformation and tetrahedron decomposition

As before, we note that any gauge transformation of the form $\mathcal{P}(i, i+2) \rightarrow \tilde{\mathcal{P}}(i, i+2) = L_i \mathcal{P}(i, i+2) L_{i+2}^{-1}$ and such that $(L_i)_{1,j} = (L_i)_{j,1} = \delta_{j,1}$ leaves the formula (3.5) invariant.

We choose

$$L_i = \begin{pmatrix} 1 & 0 & 0 \\ 0 & T_{1,i,0} & 0 \\ 0 & 0 & T_{2,i,1} \end{pmatrix}$$

Defining

$$M(a, b, c, u, v, w) = \begin{pmatrix} \frac{b}{c} & & \frac{1}{w} & 0 \\ \frac{u}{c} & \frac{u}{bc} + \frac{au}{bv} + \frac{a}{vw} & \frac{a}{w} & \frac{a}{w} \\ 0 & & \frac{1}{w} & \frac{v}{w} \end{pmatrix}$$

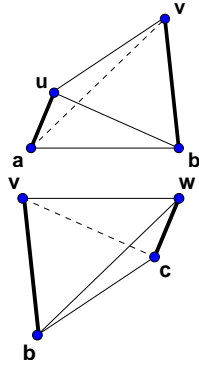
we have

$$\tilde{\mathcal{P}}(i, i+2) = M(T_{1,i,0}, T_{1,i+1,1}, T_{1,i+2,0}, T_{2,i,1}, T_{2,i+1,0}, T_{2,i+2,1})$$

The matrix M may be further decomposed as follows:

$$M(a, b, c, u, v, w) = A(a, b, u, v)B(b, c, v, w)$$

where



$$A(a, b, u, v) = \begin{pmatrix} 1 & 0 & 0 \\ \frac{u}{b} & \frac{au}{bv} & \frac{a}{v} \\ 0 & 0 & 1 \end{pmatrix}$$

$$B(b, c, v, w) = \begin{pmatrix} \frac{b}{c} & \frac{1}{c} & 0 \\ 0 & 1 & 0 \\ 0 & \frac{1}{w} & \frac{v}{w} \end{pmatrix}$$

In view of our interpretation of the boundary (see Fig.3.1), the matrices A and B may be associated to the tetrahedrons A and B. The arguments are the values of T at the vertices of the tetrahedrons. We write

$$A(i, i+1) = A(T_{1,i,1}, T_{1,i+1,0}, T_{2,i,0}, T_{2,i+1,1}) \text{ and } B(i, i+1) = B(T_{1,i,0}, T_{1,i+1,1}, T_{2,i,1}, T_{2,i+1,0})$$

and finally we may rewrite (3.5) as:

$$T_{1,j,k} = T_{1,j+k,0} \left(\prod_{i=0}^{k-1} A(j-k+2i, j-k+2i+1) B(j-k+2i+1, j-k+2i+2) \right)_{1,1} \quad (3.6)$$

We may now interpret this result as a generalization of the frieze result. By analogy with the frieze solution, let us define the projection of $(1, j, k)$ on the boundary as the portion of the boundary between the edge f_{j-k+1} and the edge f_{j+k-1} . We have:

Theorem 3.2. *The general solution of the A_2 T -system with the basic staircase boundary for $\alpha = 1$ reads:*

$$T_{1,j,k} = T_{1,j+k-1,1} \left(\prod_{i=0}^{k-2} B(j-k+2i+1, j-k+2i+2) A(j-k+2i+2, j-k+2i+3) \right)_{1,1} \quad (3.7)$$

Proof. We start from (3.6) and use the fact that $A(a, b, u, v)_{1,j} = bB(a, b, u, v)_{j,1} = \delta_{j,1}$ to eliminate the first (A) and last (B) matrices in the product on the r.h.s. \square

The product extends over the sequence of tetrahedrons along the projection of $(1, j, k)$ onto the boundary. We may think of the two tetrahedron matrices A, B as a generalization of the horizontal and vertical matrices of the A_1 case, but more general boundaries involve four more such matrices, as discussed below.

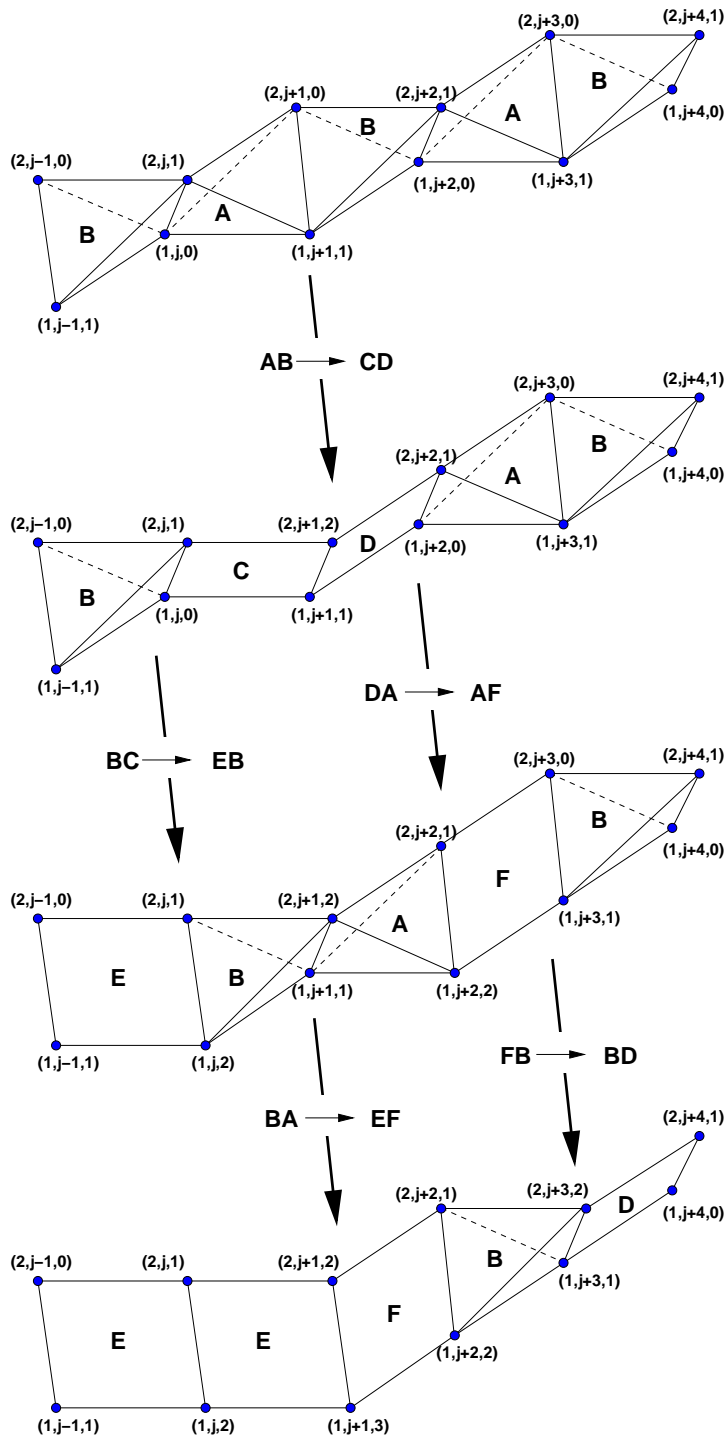


Figure 3.2: Various mutations of the basic staircase boundary for the A_2 T-system. We have indicated the tetrahedrons A,B and the parallelograms C,D,E,F that may connect two consecutive edges of the boundary.

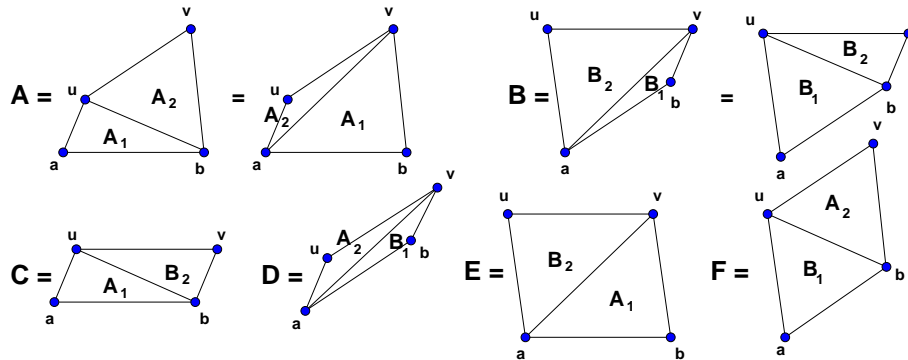


Figure 3.3: Triangle decomposition A_1, A_2, B_1, B_2 of the tetrahedrons A, B and parallelograms C, D, E, F . We use the same letter for different triangles that share the same transfer matrices (see eq.(3.10)).

3.6 Other boundaries

The most general boundaries are obtained from the basic staircase via local elementary moves (forward/backward mutations) corresponding to one application of one of the system relations. The effect is of flipping a single thick edge of the boundary in the following manner: denoting by $e_{j,k} = (1, j, k) - (2, j, k + 1)$ and $f_{j,k} = (1, j, k + 1) - (2, j, k)$, we have the two possible elementary (forward) moves:

$$\dots, e_{j,k}, \dots \rightarrow \dots f_{j,k+1} \dots \quad (3.8)$$

$$\dots, f_{j,k}, \dots \rightarrow \dots e_{j,k+1} \dots \quad (3.9)$$

It is easy to see that this gives rise to six possible relative positions for two consecutive edges:

$$(e_{j,k}, f_{j+1,k}), (f_{j,k}, e_{j+1,k}), (e_{j,k}, e_{j+1,k+1}), (e_{j,k}, e_{j+1,k-1}), (f_{j,k}, f_{j+1,k+1}), (f_{j,k}, f_{j+1,k-1})$$

which define two tetrahedrons and four parallelograms, respectively denoted by A, B and C, D, E, F (see Fig.3.2).

Note that the boundary is entirely specified by a Motzkin path and the edge at one of its vertices. Indeed the transition from an edge to the next changes $k \rightarrow k, k + 1$ or $k - 1$, and the nature of the edge (e or f) is switched only if k is unchanged. So keeping a record of the variable k is sufficient, and the record is a Motzkin path (or equivalently an infinite word in 3 letters).

3.7 Triangle decomposition

As already mentioned, we may further decompose the tetrahedrons A and B , as well as the parallelograms C, D, E, F , into pairs of triangles, as indicated in Fig.3.3. To all triangles labelled A_1, A_2, B_1, B_2 , we associate the following 3×3 “triangle” matrices with

3 parameters equal to the values of $T_{\alpha,j,k}$ at their vertices. We have:

$$\begin{aligned} A_1(a, b, u) &= \begin{pmatrix} 1 & 0 & 0 \\ \frac{u}{b} & \frac{a}{b} & 0 \\ 0 & 0 & 1 \end{pmatrix} & A_2(b, u, v) &= \begin{pmatrix} 1 & 0 & 0 \\ 0 & \frac{u}{v} & \frac{b}{v} \\ 0 & 0 & 1 \end{pmatrix} \\ B_1(a, b, u) &= \begin{pmatrix} \frac{a}{b} & \frac{1}{b} & 0 \\ 0 & 1 & 0 \\ 0 & 0 & 1 \end{pmatrix} & B_2(b, u, v) &= \begin{pmatrix} 1 & 0 & 0 \\ 0 & 1 & 0 \\ 0 & \frac{1}{v} & \frac{u}{v} \end{pmatrix} \end{aligned} \quad (3.10)$$

The two tetrahedrons A,B, correspond to the matrices

$$\begin{aligned} A(a, b, u, v) &= A_1(a, b, u)A_2(b, u, v) = A_2(a, u, v)A_1(a, b, v) \\ B(a, b, u, v) &= B_1(a, b, u)B_2(b, u, v) = B_2(a, u, v)B_1(a, b, v) \end{aligned} \quad (3.11)$$

independent of the two triangle decompositions. The parallelograms C,D,E,F of Fig.3.3 have unique triangle decompositions, to which we attach the following matrices:

$$\begin{aligned} C(a, b, u, v) &= A_1(a, b, u)B_2(b, u, v) = \begin{pmatrix} 1 & 0 & 0 \\ \frac{u}{b} & \frac{a}{b} & 0 \\ 0 & \frac{1}{v} & \frac{u}{v} \end{pmatrix} \\ D(a, b, u, v) &= A_2(a, u, v)B_1(a, b, v) = \begin{pmatrix} \frac{a}{b} & \frac{1}{b} & 0 \\ 0 & \frac{u}{v} & \frac{a}{v} \\ 0 & 0 & 1 \end{pmatrix} \\ E(a, b, u, v) &= B_2(a, u, v)A_1(a, b, v) = \begin{pmatrix} 1 & 0 & 0 \\ \frac{v}{b} & \frac{a}{b} & 0 \\ \frac{1}{b} & \frac{a}{bv} & \frac{u}{v} \end{pmatrix} \\ F(a, b, u, v) &= B_1(a, b, u)A_2(b, u, v) = \begin{pmatrix} \frac{a}{b} & \frac{u}{bv} & \frac{1}{v} \\ 0 & \frac{u}{v} & \frac{b}{v} \\ 0 & 0 & 1 \end{pmatrix} \end{aligned}$$

Note that the products are taken in a specific order, namely that the matrix for the triangle which lies on the left of the diagonal of the parallelogram multiplies that on the right from the left.

3.8 Mutations via triangles and the general formula

The general formula for $T_{1,j,k}$ for an arbitrary boundary reads as follows. First, we may view the boundary above in yet another manner, by projecting it vertically onto the bottom plane, as illustrated in Fig. 3.4. It is the superimposition of the two sets of boundary vertices in the bottom (resp. top) layers (represented as filled (resp. empty) circles), which are both staircase boundaries of the type considered in the A_1 case, drawn on the two corresponding shifted square lattice layers in thick (resp. dashed) lines. These two staircases are constrained by the condition that their vertices must be connected via e or f edges only (diagonal thick black lines in Fig.3.4).

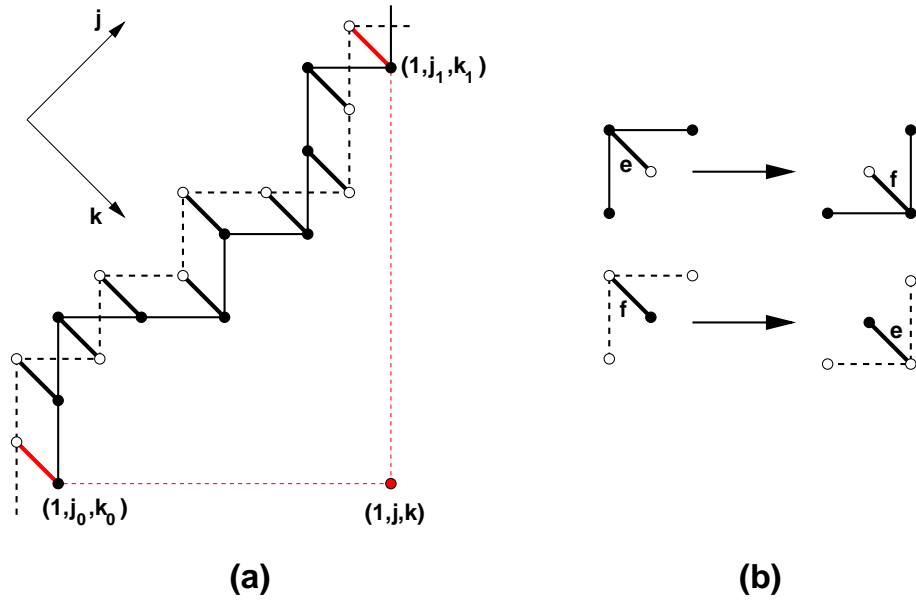


Figure 3.4: The projection of a point $(1, j, k)$ onto a typical boundary for the A_2 T-system (a), viewed in vertical projection onto the bottom plane. The vertices of the bottom (rep. top) layers are represented as filled (resp. empty) circles. The boundary edges are represented as thick diagonal lines. We have indicated (b) the two types of forward mutations corresponding to $e \rightarrow f$ and $f \rightarrow e$ as in (3.8-3.9).

Definition 3.3. *The projection of the point $(1, j, k)$ onto the boundary is the portion of boundary (finite sequence of edges) between the edges containing $(1, j_0, k_0)$ and $(1, j_1, k_1)$, respectively such that $j_0 - k_0 = j - k$ and $j_1 + k_1 = j + k$ with j_0 maximal and j_1 minimal.*

This coincides with the definition for the A_1 T-system, using the staircase of the bottom layer only. The corresponding finite sequence of edges corresponds alternatively to a finite sequence of triangles according to the decomposition above, modulo the two-fold ambiguities of decomposition of the tetrahedrons A and B.

To this sequence we associate the matrix:

$$M(j, k) = \prod_{\substack{\text{triangle } Z \\ \text{w/vertex values } x, y, z}} Z(x, y, z) \quad (3.12)$$

where for each triangle $Z=A_1, A_2, B_1, B_2$, along the sequence we multiply by the corresponding triangle matrix $Z = A_1, A_2, B_1, B_2$. Note that, due to the identities (3.11), this definition is independent of the particular choice of triangle decomposition of the possible tetrahedrons along the boundary. We have:

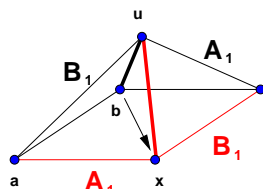
Theorem 3.4. *The solution of the A_2 T-system for arbitrary boundary reads for $\alpha = 1$:*

$$T_{1,j,k} = T_{1,j_1,k_1} M(j, k)_{1,1} \quad (3.13)$$

with $M(j, k)$ as in (3.12), with the product extending over the projection of $(1, j, k)$ onto the boundary.

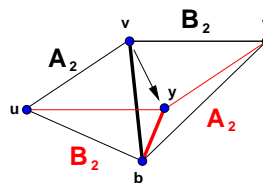
Before proving the Theorem by induction under mutation, let us describe the mutations of the boundary in more detail. The two possible mutations (3.8-3.9) correspond to a local transformation of the chain of triangles that forms the boundary, namely it replaces a pair of adjacent triangles sharing the initial boundary edge with a new pair of adjacent triangles sharing the mutated boundary edge. Using the definition (3.10), we get the following Lemma, generalizing Lemma 2.6:

Lemma 3.5. *For all $a, b, c, u, v, w > 0$ we have:*



$$B_1(a, b, u)A_1(b, c, u) = A_1(a, x, u)B_1(x, c, u), \quad (3.14)$$

$(bx = ac + u)$



$$A_2(b, u, v)B_2(b, v, w) = B_2(b, u, y)A_2(b, y, w), \quad (3.15)$$

$(vy = uw + b)$

where we have represented in thick black (resp. red) line the initial (resp. mutated) boundary edge.

In the above equations, the transformations $b \rightarrow x$ (resp. $v \rightarrow y$) are precisely the two types of forward mutations of the A_2 T-system cluster algebra, obtained by applying the first (resp. second) line of (3.1). We may now turn to the proof of Theorem 3.4.

Proof. The formula is proved by induction under mutation. We start from the basic staircase solution (3.7), which may be put in the form (3.13), upon substituting $A = A_1A_2$ and $B = B_1B_2$, and noting that $k_1 = 1$, $j_1 = j + k - 1$, while $k_0 = 1$ and $j_0 = j - k + 1$.

Starting from the expression (3.13) for the basic staircase boundary, we may apply iteratively either of (3.14) or (3.15) to get to any other boundary (up to global translation), by simply substituting products of pairs of triangle matrices into the expression (3.13).

We must however pay special attention to the extremal cases, namely when the mutation acts on the edge just before the upper extremity as in Fig.3.5 (a), or just after the lower extremity as in Fig.3.5 (b), of the projection of $(1, j, k)$.

The prefactor T_{1,j_1,k_1} in (3.13) corresponds indeed to the bottom vertex of the upper extremity of the projection of $(1, j, k)$ onto the boundary. Assuming as in Fig.3.5 (a) that the edge just before the upper extremity of the projection of $(1, j, k)$ is of e type, with value b at the bottom vertex as in eq. (3.14), the mutation sends it to an f -type edge with bottom vertex value x , which becomes the new upper extremity of the projection of $(1, j, k)$, replacing c . Noting that $B_1(x, c, u)_{j,1} = \delta_{j,1} \frac{x}{c}$, we see that the last multiplication by $B_1(x, c, u)$ amounts to replacing the global prefactor c by x , which is the desired change of T_{1,j_1,k_1} . Analogously, when the mutation acts on an edge of type e next to the bottom extremity of the projection as in Fig.3.5 (b), with bottom vertex value b as in (3.14),

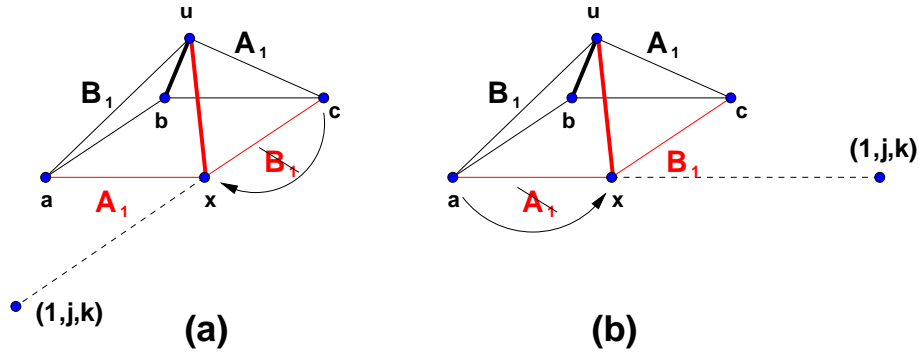


Figure 3.5: The effect of a mutation next to the top (a) and bottom (b) of the projection of $(1, j, k)$. The new mutated edge is represented in red. The corresponding new lower vertex of the projection extremity is changed accordingly: $c \rightarrow x$ (a) and $a \rightarrow x$ (b). The extremal matrices $B_1(x, c, u)$ (a) and $A_1(a, x, u)$ (b) must be dropped from the expression for $M(i, j)$, as the corresponding triangles lie outside of the new projection of $(1, j, k)$.

it sends it to an edge of type f with bottom value x , which becomes the new lower extremity of the projection of $(1, j, k)$, replacing a . As $A_1(a, x, u)_{1,j} = \delta_{j,1}$, we may drop the contribution of this first triangle, and we recover (3.13). This completes the proof of the Theorem. \square

The case $\alpha = 2$ needs no extra work, due to the following symmetry:

Lemma 3.6. *For any fixed boundary, with initial data of the form $\{T_{\alpha,j,k_{\alpha,j}}\}_{\alpha=1,2;j \in \mathbb{Z}}$ we have*

$$T_{2,j,k}(\{T_{\alpha,j,k_{\alpha,j}}\}_{\alpha=1,2;j \in \mathbb{Z}}) = T_{1,j,k}(\{T_{3-\alpha,j,k_{3-\alpha,j}}\}_{\alpha=1,2;j \in \mathbb{Z}})$$

Proof. The transformation $\alpha \rightarrow r + 1 - \alpha$ is a symmetry of (1.1-1.2). \square

Corollary 3.7. *The solution of the A_2 T-system for arbitrary boundary is for all $\alpha = 1, 2$ a Laurent polynomial of the initial data with non-negative integer coefficients.*

4 The A_r case

4.1 T-system

We now consider the general A_r T-system (1.1-1.2) for $j, k \in \mathbb{Z}$, and $\alpha \in I_r$. As before, this splits again into two independent systems for $T_{\alpha,j,k}$ with fixed value of $\alpha + j + k$ modulo 2, which we fix to be 0, without loss of generality.

The indices $\{(\alpha, j, k)\}$ for $\alpha + j + k = 0$ modulo 2 run over r consecutive horizontal layers $\alpha = 1, 2, \dots, r$ of the centered cubic lattice, each of which is a square lattice, the vertices of the next layer lying at the vertical of the centers of the faces of the previous one. For technical reasons, we will also represent the extra bottom and top layers $\alpha = 0$ and $\alpha = r + 1$, within which all values of T are fixed to 1, by the A_r boundary condition (1.2).

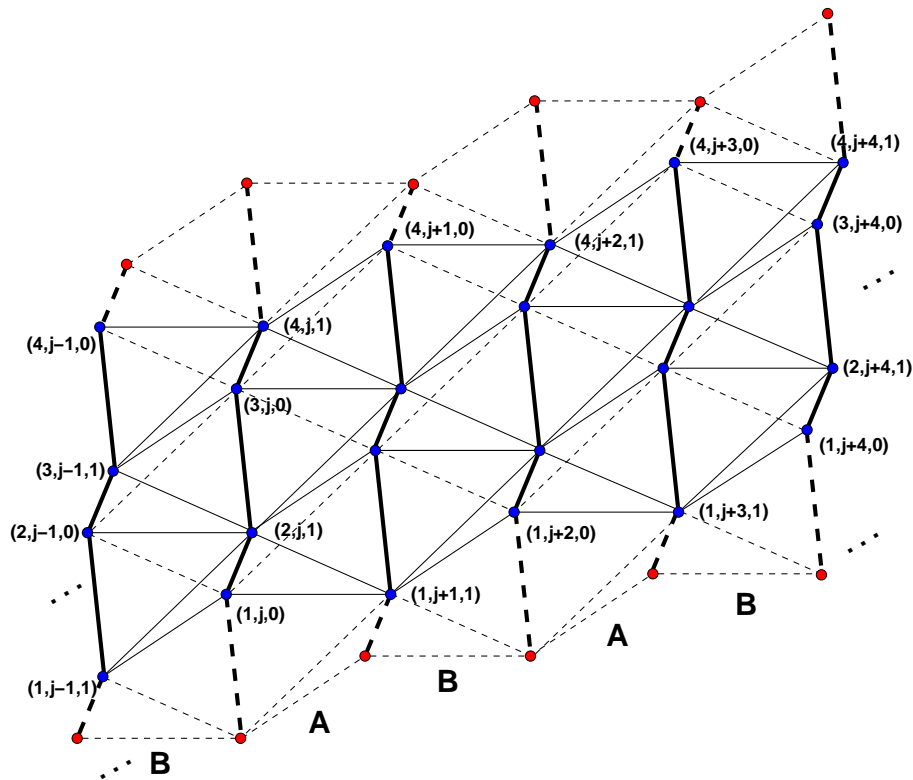


Figure 4.1: The basic staircase boundary for the A_r T-system, here for $r = 4$, on which all vertex values $T_{\alpha,j,0}$ and $T_{\alpha,j-1,1}$ are specified (blue dots). We have added an extra bottom and top layer where, according to the A_r boundary, all vertex values are set to 1 (red dots).

4.2 Boundaries

As before we start with the basic boundary $\{T_{\alpha,j,0}, T_{\alpha,j-1,1}\}_{\alpha \in I_r, j \in \mathbb{Z}}$ for $\alpha + j$ even. We may describe this boundary in 3D space as a succession of broken lines at constant j (represented in thick solid lines in Fig.4.1) of the form:

$$\ell_j = \{(\alpha, j, \epsilon_{\alpha,j})\}_{\alpha=1}^r, \quad \epsilon_{\alpha,j} = \alpha + j \pmod{2} \quad (4.1)$$

We denote by A,B the vertical stacks of tetrahedrons depicted in Fig.4.1, respectively between ℓ_{2i-1} and ℓ_{2i} and ℓ_{2i} and ℓ_{2i+1} for all $i \in \mathbb{Z}$. Each tetrahedron has two opposite (thick) edges of the form $(\alpha, j, \epsilon) - (\alpha + 1, j, 1 - \epsilon)$ and $(\alpha, j + 1, 1 - \epsilon) - (\alpha + 1, j + 1, \epsilon)$.

4.3 Solution for the basic staircase boundary

In Ref. [7], the system was solved for the basic staircase boundary in two steps. First one eliminates $T_{\alpha,j,k}$ for all $\alpha > 1$ as:

$$T_{\alpha,j,k} = \det_{1 \leq a, b \leq \alpha} (T_{1, j-a+b, k+a+b-\alpha-1}), \quad \alpha \in I_r, \quad j, k \in \mathbb{Z} \quad (4.2)$$

which allows to concentrate on $T_{1,j,k}$.

The solution $T_{1,j,k}$ was then expressed in terms of paths on a rooted target graph with time-dependent weights involving only the boundary values. More precisely, $T_{1,j,k}$ was found to be equal to $T_{1,j+k,0}$ times the partition function for paths starting from the root at time $j - k$ and ending at the root at time $j + k$. It is best expressed in terms of the $2r + 2 \times 2r + 2$ transfer matrix, encoding the step weights $\mathbf{y} = y_1, y_2, \dots, y_{2r+1}$:

$$\mathcal{T}(\mathbf{y}) = \begin{pmatrix} 0 & 1 & 0 & 0 & 0 & \cdots & 0 & 0 & 0 & 0 \\ y_1 & 0 & 1 & 0 & 0 & \cdots & 0 & 0 & 0 & 0 \\ 0 & y_2 & 0 & 1 & 1 & \cdots & 0 & 0 & 0 & 0 \\ 0 & 0 & y_3 & 0 & 0 & \cdots & 0 & 0 & 0 & 0 \\ 0 & 0 & y_4 & 0 & 0 & \cdots & 0 & 0 & 0 & 0 \\ \vdots & \vdots & & & & \ddots & & & & \vdots \\ 0 & 0 & 0 & 0 & 0 & \cdots & 0 & 1 & 1 & 0 \\ 0 & 0 & 0 & 0 & 0 & \cdots & y_{2r-1} & 0 & 0 & 0 \\ 0 & 0 & 0 & 0 & 0 & \cdots & y_{2r} & 0 & 0 & 1 \\ 0 & 0 & 0 & 0 & 0 & \cdots & 0 & 0 & y_{2r+1} & 0 \end{pmatrix}$$

Defining the time-dependent weights

$$y_1(t) = \frac{T_{1,t,1}}{T_{1,t+1,0}}, \quad y_{2\alpha+1}(t) = \frac{T_{\alpha+1,t-1,1} T_{\alpha,t+1,0}}{T_{\alpha+1,t,0} T_{\alpha,t,1}}, \quad y_{2\alpha}(t) = \frac{T_{\alpha+1,t,1} T_{\alpha-1,t+1,0}}{T_{\alpha,t,0} T_{\alpha,t+1,1}}, \quad (\alpha = 1, 2, \dots, r)$$

and the transfer matrix for steps from time t to $t + 1$:

$$\mathcal{T}(t, t + 1) = \mathcal{T}(y_1(t), y_2(t), \dots, y_{2r+1}(t))$$

we have:

Theorem 4.1 ([7]). *The solution of the A_r T -system (1.1-1.2) for the basic staircase boundary reads for $\alpha = 1$:*

$$T_{1,j,k} = T_{1,j+k,0} \left(\prod_{t=j-k}^{j+k-1} \mathcal{T}(t, t + 1) \right)_{1,1}$$

4.4 Reduced transfer matrix

As before we note that the two-step transfer matrix $\mathcal{P}(\mathbf{y}, \mathbf{y}') = \mathcal{T}(\mathbf{y})\mathcal{T}(\mathbf{y}')$ is again decomposable into two linear operators acting on two complementary spaces of dimensions $r + 1$, corresponding respectively to components $(1, 3, 6, 7, 10, 11, \dots)$ and $(2, 4, 5, 8, 9, \dots)$. Explicitly, the operator acting on the first set of components reads:

$$\mathcal{P}(\mathbf{y}, \mathbf{y}') = \begin{pmatrix} y'_1 & 1 & 0 & 0 & 0 & 0 & 0 & \cdots \\ y_2 y'_1 & y_2 + y'_3 + y'_4 & 1 & 1 & 0 & 0 & 0 & \\ 0 & y_5 y'_4 & y_5 & y_5 & 0 & 0 & 0 & \\ 0 & y_6 y'_4 & y_6 & y_6 + y'_7 + y'_8 & 1 & 1 & 0 & \\ 0 & 0 & 0 & y_9 y'_8 & y_9 & y_9 & 0 & \\ 0 & 0 & 0 & y_{10} y'_8 & y_{10} & y_{10} + y'_{11} + y'_{12} & 1 & \\ \vdots & & & & & \ddots & & \end{pmatrix}$$

The corresponding reduced two-step transfer matrix is $\mathcal{P}(t, t + 2) = \mathcal{P}(\mathbf{y}(t), \mathbf{y}(t + 1))$. Theorem 4.1 turns into:

$$T_{1,j,k} = T_{1,j+k,0} \left(\prod_{i=0}^{k-1} \mathcal{P}(j - k + 2i, j - k + 2i + 2) \right)_{1,1} \quad (4.3)$$

4.5 Gauge transformation and rhombus/triangle decomposition

We may apply to \mathcal{P} any gauge transformation of the form $\tilde{\mathcal{P}}(t, t + 2) = L_t \mathcal{P}(t, t + 2) L_{t+2}^{-1}$ and such that $(L_t)_{1,j} = (L_t)_{j,1} = \delta_{j,1}$ without altering the result (4.3).

Here we choose:

$$L_t = \text{diag}\left(1, T_{1,t,0}, \frac{T_{2,t,1} T_{3,t,0}}{T_{3,t-1,1}}, T_{3,t,0}, \dots, T_{2\alpha-1,t,0}, \frac{T_{2\alpha,t,1} T_{2\alpha+1,t,0}}{T_{2\alpha+1,t-1,1}}, \dots\right)$$

One advantage of this choice is that $\tilde{\mathcal{P}}(t, t + 2)$ only depends on values of $T_{\alpha,j,k}$ at times $j = t, t + 1, t + 2$. It is also justified *a posteriori* by the decomposition formulas below.

We will now decompose the reduced two-step transfer matrix $\tilde{\mathcal{P}}$ into a product of elementary matrices, defined as follows.

Definition 4.2. We define the following 2×2 elementary step matrices:

$$H(a, b, x) = \begin{pmatrix} 1 & 0 \\ \frac{x}{b} & \frac{a}{b} \end{pmatrix} \quad V(x, a, b) = \begin{pmatrix} \frac{a}{b} & \frac{x}{b} \\ 0 & 1 \end{pmatrix} \quad (4.4)$$

Note that these generalize the horizontal and vertical step matrices of Definition 2.2, used in the A_1 case.

Definition 4.3. For any 2×2 matrix X and $\alpha \in \{1, 2, \dots, r\}$ define the $r + 1 \times r + 1$ matrices:

$$X_{\alpha,\alpha+1} = \left(\begin{array}{c|c|c} 1_{\alpha-1} & 0_{\alpha-1 \times 2} & 0_{\alpha-1 \times r-\alpha} \\ \hline 0_{2 \times \alpha-1} & X & 0_{2 \times r-\alpha} \\ \hline 0_{r-\alpha \times \alpha-1} & 0_{r-\alpha \times 2} & 1_{r-\alpha} \end{array} \right) \quad (4.5)$$

where 1_m denotes the $m \times m$ identity matrix and $0_{m \times p}$ the $m \times p$ matrix with zero entries.

This gives rise to matrices $H_{\alpha,\alpha+1}(a, b, u)$ and $V_{\alpha,\alpha+1}(a, x, y)$ using for X (4.5) the matrices (4.4). As an example, the triangle matrices A_1, A_2, B_1, B_2 introduced in the A_2 case (3.10) may be identified with:

$$\begin{aligned} A_1(a, b, u) &= H_{1,2}(a, b, u) & A_2(b, u, v) &= V_{2,3}(b, u, v) \\ B_1(a, b, u) &= V_{1,2}(1, a, b) & B_2(b, u, v) &= H_{2,3}(u, v, 1) \end{aligned}$$

We finally define:

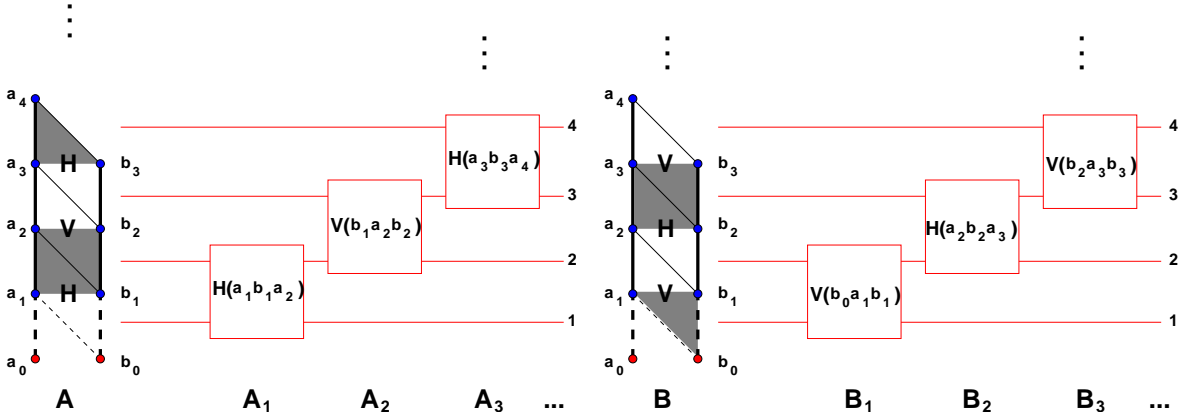


Figure 4.2: The triangle decomposition of the stacks A, B of tetrahedrons on the basic staircase boundary. The triangles are colored either white or gray, and are grouped into pairs of distinct colors sharing an edge (rhombi). The H (resp. V) rhombi have the gray triangle pointing up (resp. down), and correspond to products with the matrices H (resp. V) in the indicated manner. The three parameters are the values of $T_{\alpha, j, k}$ at the vertices of the gray triangle.

Definition 4.4. We define the following $r + 1 \times r + 1$ matrices:

$$A_\alpha(a, x, y, u) = \begin{cases} H_{\alpha, \alpha+1}(x, y, u) & \text{if } \alpha \text{ odd} \\ V_{\alpha, \alpha+1}(a, x, y) & \text{if } \alpha \text{ even} \end{cases} \quad (4.6)$$

$$B_\alpha(a, x, y, u) = \begin{cases} V_{\alpha, \alpha+1}(a, x, y) & \text{if } \alpha \text{ odd} \\ H_{\alpha, \alpha+1}(x, y, u) & \text{if } \alpha \text{ even} \end{cases} \quad (4.7)$$

and for sequences $\mathbf{a} = a_0, a_1, \dots, a_{r+1}$ and $\mathbf{b} = b_0, b_1, \dots, b_{r+1}$, we define:

$$\begin{aligned} A(\mathbf{a}; \mathbf{b}) &= A_1(b_0, a_1, b_1, a_2) A_2(b_1, a_2, b_2, a_3) \dots A_r(b_{r-1}, a_r, b_r, a_{r+1}) \\ B(\mathbf{a}; \mathbf{b}) &= B_1(b_0, a_1, b_1, a_2) B_2(b_1, a_2, b_2, a_3) \dots B_r(b_{r-1}, a_r, b_r, a_{r+1}) \end{aligned} \quad (4.8)$$

Theorem 4.5. The following decomposition holds:

$$\tilde{\mathcal{P}}(t, t+2) = A(\mathbf{a}(t), \mathbf{a}(t+1)) B(\mathbf{a}(t+1), \mathbf{a}(t+2))$$

where $a_\alpha(t) = T_{\alpha, t, \epsilon_{\alpha, t}}$, with $\epsilon_{\alpha, t}$ as in (4.1), and in particular $a_0(t) = a_{r+1}(t) = 1$, due to the A_r boundary condition.

Proof. By direct calculation. □

In analogy with the frieze result, we may now interpret pictorially the decomposition result above. We interpret the matrices $A(\mathbf{a}(j-1), \mathbf{a}(j))$ and $B(\mathbf{a}(j), \mathbf{a}(j+1))$ as corresponding respectively to the stacks A, B of tetrahedrons in Fig.4.1. Each tetrahedron may be decomposed in two ways into a pair of triangles (the thin solid lines in Fig.4.1 correspond to one particular choice for each tetrahedron).

Let us now pick the canonical choice indicated in Fig.4.2 for both types A, B of stacks, namely that all squares are divided along their second diagonal. Then each term A_i or B_i

in the products (4.8) may be associated to a pair of triangles sharing an horizontal edge (which we call a rhombus, by a slight abuse).

As illustrated in Fig.4.2, we color the triangles in white or gray in such a way that rhombi are made of one triangle of each color. This gives rise to two types of rhombi H (resp. V), depending on whether the gray triangle is on top (resp. bottom), that are interchanged when going from stacks of type A to type B. In the rhombi, gray triangles play a particular role: their vertex values carry the 3 parameters of respectively the matrices H or V in the product definition of A_i or B_i (4.6-4.7). Taking the product over the rhombi from bottom to top yields the formulas (4.8).

Each stack contains $r - 1$ tetrahedrons, hence there are 2^{r-1} possible triangle/rhombus decompositions of each stack of type A (resp. B), each made of r rhombi. By their definition (4.5-4.6-4.7), the operators A_i and A_j (resp. B_i and B_j) commute as soon as $|i - j| > 1$. So a given rhombus decomposition carries the information of whether A_i multiplies A_{i+1} from the left (like in Fig.4.2) or from the right (for the other choice of diagonal in the i -th tetrahedron from the bottom), and of what the three arguments of the H or V factors are (via the boundary values at the vertices of the gray triangle).

The 2^{r-1} *a priori* distinct matrix products corresponding to these rhombus decompositions turn out to be identical. This is a consequence of the following local commutation relations (for odd i):

$$\begin{aligned} A_{i-1}(x, a, b, a')A_i(b, a', b', y) &= A_i(a, a', b', y)A_{i-1}(x, a, b, b') \\ B_{i-1}(x, a, b, a')B_i(b, a', b', y) &= B_i(a, a', b', y)B_{i-1}(x, a, b, b') \end{aligned}$$

easily derived from the following:

Lemma 4.6.

$$H_{i-1,i}(a, b, a') V_{i,i+1}(b, a', b') = V_{i,i+1}(a, a', b') H_{i-1,i}(a, b, b') \quad (4.9)$$

$$V_{i-1,i}(x, a, b) H_{i,i+1}(a', b', y) = H_{i,i+1}(a', b', y) V_{i-1,i}(x, a, b) \quad (4.10)$$

Proof. By direct computation. □

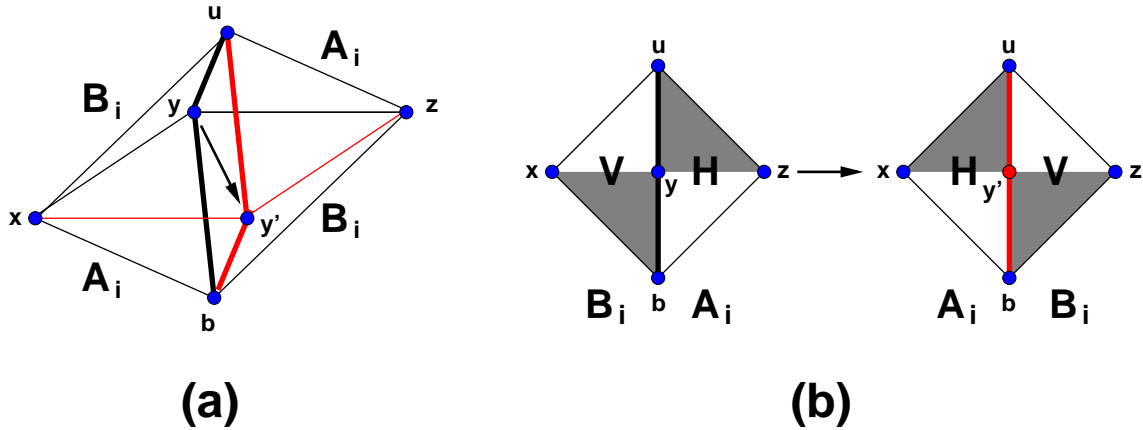


Figure 4.3: A forward mutation of the boundary consists of a vertex value update $y \rightarrow y'$, with $yy' = xz + au$. It takes the 4 triangles in the back (black lines) of the octahedron (a) to the 4 triangles in the front (red lines). We have also represented (b) the corresponding A_i - B_i matrix identity, equivalent to a rhombus exchange, in the case of odd i .

Theorem 4.1 now turns into:

$$T_{1,j,k} = T_{1,j+k,0} \left(\prod_{i=0}^{k-1} A(\mathbf{a}(j-k+2i), \mathbf{a}(j-k+2i+1)) B(\mathbf{a}(j-k+2i+1), \mathbf{a}(j-k+2i+2)) \right)_{1,1} \quad (4.11)$$

With the above-mentioned freedom of picking any of the 2^{r-1} A and B product decompositions for each transfer matrix $A(\mathbf{a}(t), \mathbf{a}(t+1))$ and $B(\mathbf{a}(t+1), \mathbf{a}(t+2))$ in (4.11), we get $2^{k(r-1)}$ equivalent expressions for $T_{1,j,k}$.

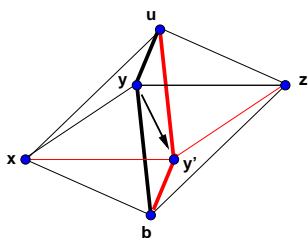
4.6 Mutations as rhombus exchange

Forward mutations of the boundary of the A_r T-system may take place whenever five neighboring vertices form the back of an octahedron, say in positions $(i, j, k-1)$, $(i, j-1, k)$, $(i, j+1, k)$, $(i-1, j, k)$ and $(i+1, j, k)$, in which case the mutation $\mu_{i,j}$ replaces the back vertex $(i, j, k-1)$ with the front one $(i, j, k+1)$. It also induces the update of the boundary value y of the back vertex with $y' = \frac{bu+xz}{y}$ for the front one (see Fig.4.3 (a), with $x = T_{i,j-1,k}$, $y = T_{i,j,k-1}$, $z = T_{i,j+1,k}$, $b = T_{i-1,j,k}$, $u = T_{i+1,j,k}$, and $y' = T_{i,j,k+1}$). Backward mutations just correspond to the inverse process with $y' \rightarrow y$.

Whenever a mutation is possible, using the freedom to pick rhombus decompositions, we will see in next section that we may always bring H and V rhombi in contact. The mutation corresponds then to interchanging the two rhombi: it is a forward mutation if V passes from the left to the right of H (see Fig. 4.3), backward otherwise.

To check that the mutation is faithfully represented by the matrices, we use the following:

Lemma 4.7.



$$V(b, x, y) H(y, z, u) = H(x, y', u) V(b, y', z), \quad yy' = xz + bu$$

(4.12)

Proof. By direct calculation. □

The forward mutation $\mu_{i,j}$ is implemented by simply switching the two rhombi in the decomposition of the corresponding adjacent stacks. In the case i odd, this corresponds to the identity depicted in Fig.4.3 (b):

$$A_i(b, x, y, u) B_i(b, y, z, u) = B_i(b, x, y', u) A_i(b, y', z, u) \quad yy' = xz + bu,$$

a direct consequence of Lemma 4.7. When i is even, the mutation $\mu_{i,j}$ corresponds to the same identity read in the opposite direction (but still corresponds to a V passing from the left to the right of an H).

We conclude that the forward mutations $\mu_{i,j}$ of the boundary may be iteratively implemented on the formula (4.11) by simply (i) picking the relevant rhombus decomposition among all equivalent ones namely bring a V to the left of an H with the vertex $(i, j, k_{i,j})$ of the boundary in the center (ii) switching the corresponding matrices A_i and B_i in the product transfer matrix. This will be made very precise in the next section.

4.7 Arbitrary boundaries and the 6 Vertex model

In this section, we give a bijection between boundary strips of the A_r T-system and configurations of the 6-Vertex (6V) model on infinite strips of width $r - 1$. In the 6V picture, mutations correspond to the reversal of all spins around square faces whose spins form an oriented loop.

4.7.1 Local configurations and the six vertices

Recall that the 6V model is a statistical model defined on the square lattice, whose configurations consist of an orientation (spin) on each edge, in such a way that the following “ice rule” is satisfied: at each vertex of the lattice there are exactly two entering and two outgoing edges.

The idea of the bijection is very simple. As we noted before, the boundary strips may be decomposed into broken lines ℓ_j at time j , $j \in \mathbb{Z}$, as in (4.1), each made of a succession of $r - 1$ edges of type e or f . As discovered in the case of A_2 , there are 6 possible transitions between an edge of type e or f of the form $e = (\alpha, j, k) - (\alpha + 1, j, k + 1)$ or $f = (\alpha, j, k) - (\alpha + 1, j, k - 1)$, at time j , connecting vertices in the layers α and $\alpha + 1$, and

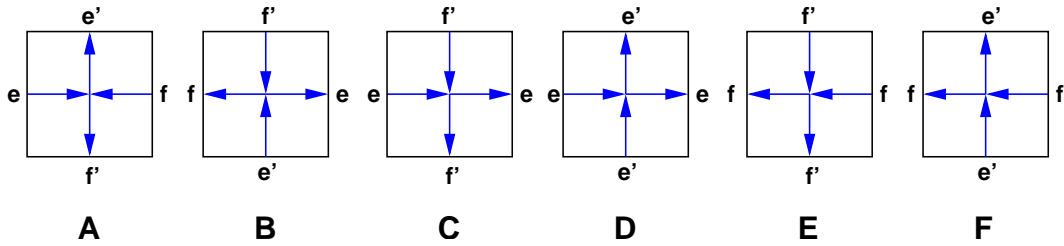


Figure 4.4: The projections in (α, j) plane of the six local configurations of the boundary of the A_r -T-system and the corresponding local arrow configurations of the dual 6V model. We have indicated for each configuration the corresponding tetrahedron (A,B) or parallelogram (C,D,E,F).

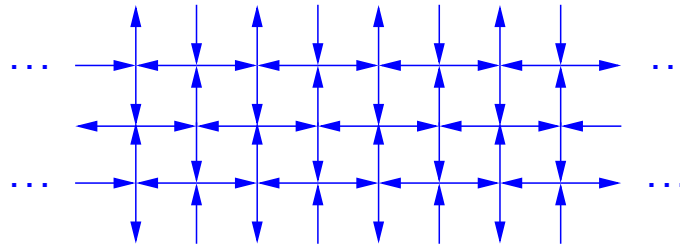


Figure 4.5: The 6V configuration corresponding to the basic staircase configuration of Fig.4.1 for $r = 4$.

an edge of either type at time $j + 1$, also connecting vertices in the layers α and $\alpha + 1$. The two corresponding edges give rise to either tetrahedrons A,B if they are of opposite types, and parallelograms C,D,E,F otherwise. Moreover, the 4 vertices included in the two edges also define two horizontal edges respectively within the layers α and $\alpha + 1$. These may also be of only two types, say e' and f' , of the form: $e' = (\alpha, j, k) - (\alpha, j + 1, k + 1)$ and $f' = (\alpha, j, k) - (\alpha, j + 1, k - 1)$.

These 6 local configurations A,B,C,D,E may be represented as squares in projection onto a (j, α) plane, with vertical edges labeled e or f and horizontal edges labeled e' or f' . In this projection, a complete boundary is simply a strip of squares, infinite in the j direction, and of finite width in the α direction, with some compatible edge assignments. The corresponding configurations of the 6V model are on the dual of this strip, namely with a vertex in the middle of each square.

To the 6 configurations of each square, we associate bijectively the 6 vertices of the 6V model as indicated in Fig.4.4, namely we pick the horizontal edge orientation to be to the right (resp. left) for an e type (resp. f type) edge, while the vertical edge is oriented upward (resp. downward) for an e' type (resp. f' type) edge.

Another direct way of connecting the initial boundary vertices to the 6V configuration is to view the latter as coding the value of $k_{\alpha, j}$ as the label of the face (j, α) in the 6V configuration as follows. Note first that values of k differ by ± 1 in neighboring faces. We impose the following ‘‘Ampère rule’’ that the value of k on the right of an arrow is smaller than that on the left. This fixes all the values of $k_{\alpha, j}$ up to a global translation.

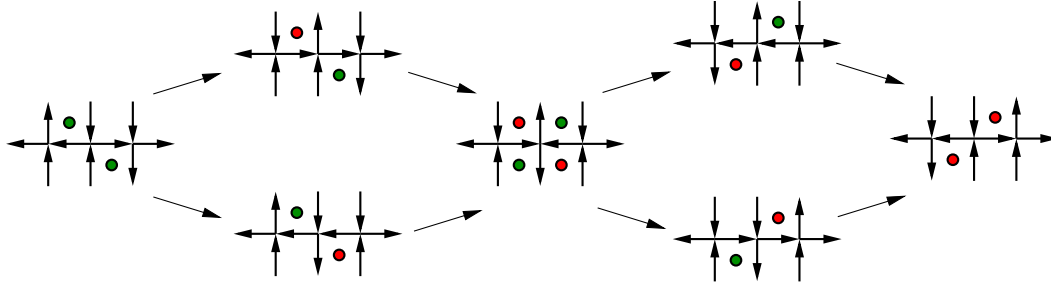


Figure 4.6: A sequence of mutations applied on a length 2 portion of the boundary strip for A_2 in the 6V formulation. The green (resp. red) dots mark the places where a forward (resp. backward) mutation can be applied. The spin of the top and bottom edge sequences are conserved, equal to -1 and 1 here.

4.7.2 The basic staircase boundary as a 6V configuration

We now consider the basic staircase boundary introduced in Section 4.2. It is an infinite horizontal strip of square lattice with height $r-1$, with an alternance of \dots, e, f, e, f, \dots vertical edges and $\dots, e', f', e', f' \dots$ horizontal edges, namely a checkerboard of configurations A and B of tetrahedrons, with vertices such that $k_{\alpha,j} \in \{0, 1\}$. The dual 6V configuration is simply made of arrows that alternate in all directions (it is a fully antiferromagnetic groundstate configuration). In particular the bottom and top horizontal rows of vertical edges alternate along the j direction.

4.7.3 Mutations as loop reversals

As illustrated in Fig.4.3, a mutation of the boundary at a given vertex amounts to transforming the 4 edges sharing this vertex, by simply permuting the two vertical ones (i.e. belonging to the plane $j = \text{const.}$) and the two horizontal ones (i.e. belonging to the plane $\alpha = \text{const.}$). This is also true if $\alpha = 1$ or $\alpha = r$, with the condition that the bottom (resp. top) vertex which belongs to the layer $\alpha = 0$ (resp. $\alpha = r + 1$) has an attached value 1. This situation was already encountered in the case $r = 1$ (see Lemma 2.6) and $r = 2$ (see Lemma 3.5).

Such a mutation can only take place if the permuted edges are of respective following types, clockwise around the vertex from the top: e, e', f, f' for a forward mutation, and f, f', e, e' for a backward mutation, and the two are transformed into one-another.

Once reformulated via the 6V bijection, and for $1 < \alpha < r$, this simply means that a forward (resp. backward) mutation can take place only around faces whose adjacent edges form a clockwise (resp. counterclockwise) oriented loop, and the mutation simply reverses the direction of all 4 arrows. When $\alpha = 1$ (resp. $\alpha = r$), the “loop” is open, i.e. is only formed of 3 edges with the bottom (resp. top) edge of the loop missing. In the case of A_1 , we are only left with open loops with both the top and bottom horizontal edges missing. In both cases, the corresponding mutation reverses the orientations of the 2 or 3 edges around the loop. By a slight abuse of language we still call “loops” these open loops, and still refer to the edge reversal as “loop reversal”.

Starting from the basic configuration of Fig.4.5, we may therefore generate all others

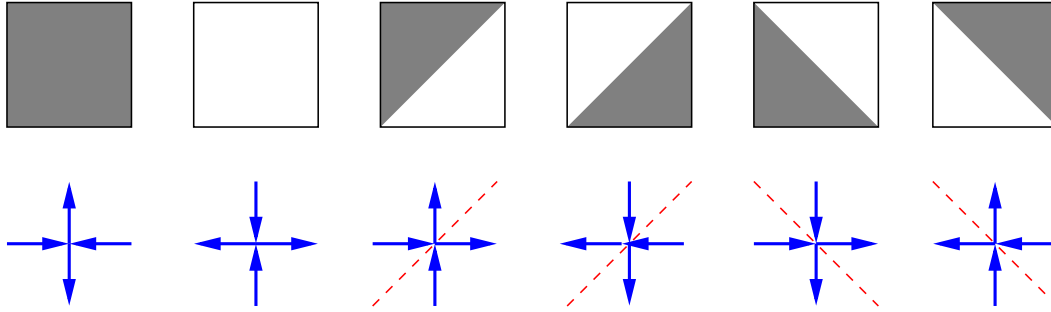


Figure 4.7: The correspondence between 6V configurations and the square/triangle decomposition of the dual lattice. The diagonals that split squares into two triangles are the diagonal reflection symmetry axes of the vertex configurations (dashed lines). Vertices without diagonal reflection symmetry correspond to squares. The gray (resp. white) triangles or squares correspond to horizontal arrows pointing toward (resp. from) the central vertex, and vertical arrows pointing from (resp. toward) the central vertex.

by successive elementary loop reversals. For illustration, we display in Fig.4.6 a sequence of mutations applied to a length 2 portion of boundary in the A_2 case. The central configuration corresponds to the basic staircase boundary.

All our 6V boundaries are generated by iterated loop reversals on the 6V basic staircase. However, the basic staircase has the particular property that its top and bottom boundary vertical edges alternate between up and down. Loop reversals involving these will create zones of successive up or down edges, with the property that the total spin (i.e. the total number of up minus down edges) remains 0. We deduce the following:

Lemma 4.8. *The boundaries of the A_r T-system correspond to the configurations of the 6V model on an infinite strip of width $r - 1$, such that there exist two times j_{min} and $j_{max} \in \mathbb{Z}$ with the same parity such that:*

- (i) *The portions of 6V boundary for $j \leq j_{min}$ and for $j \geq j_{max}$ are identical to those corresponding to the basic staircase.*
- (ii) *The total spin for the portion for $j_{min} \leq j \leq j_{max}$ of 6V boundary is zero for both top and bottom vertical edges.*

Finally, the 6V boundaries must also carry the information of the initial data: there is one initial value per vertex of the original boundary, hence these may be represented as face labels for the 6V configuration (including the bottom and top faces with only 3 bounding edges).

4.8 From general boundaries to networks

We now wish to associate transfer matrices to the 6V configurations described above.

4.8.1 6V and square/triangle decomposition

To define the transfer matrices associated to 6V configurations, we first associate to each 6V configuration a square/triangle decomposition of the dual square lattice via the

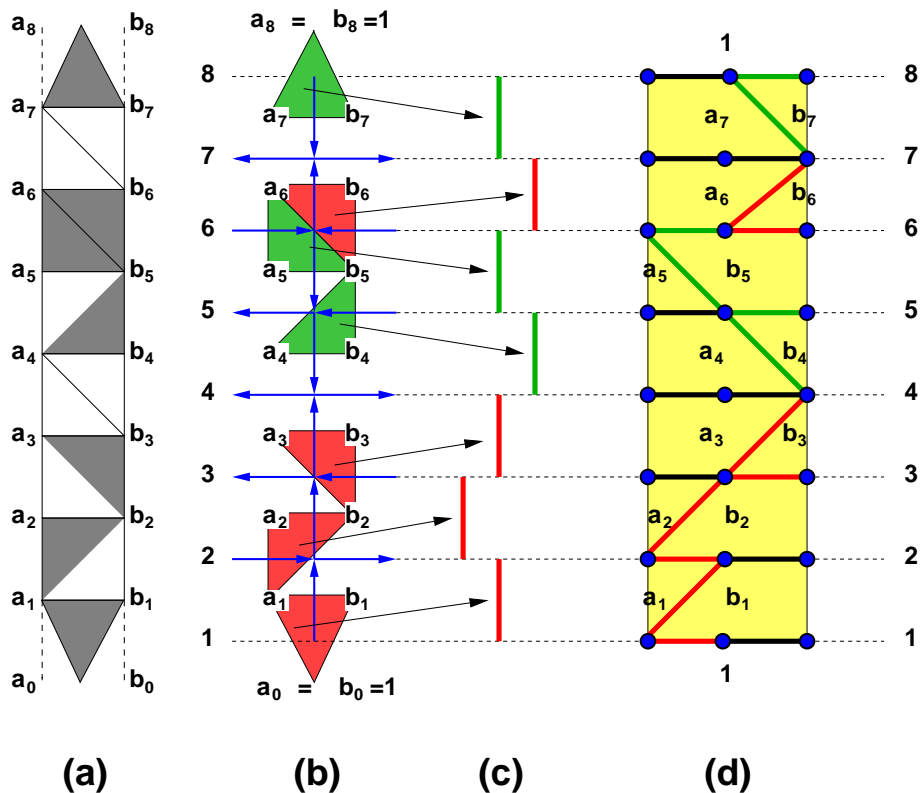


Figure 4.8: A typical vertical slice in square/triangle decomposition (a) and the associated 6V configuration (b) in the A_7 case. The squares in (a) are further cut into two triangles by drawing the second diagonal. The configurations (a)-(b) determine the H, V structure of the transfer matrix (c) where green (resp. red) segments between lines $i, i + 1$ correspond to $H_{i,i+1}$ (resp. $V_{i,i+1}$) matrices. The relative position of segments in consecutive horizontal slices corresponds to the order of multiplication of the associated matrices. We also indicate the network (d) corresponding to the complete matrix product. The labels a_i, b_i are now face labels of the network.

correspondence of Fig.4.7. Note that each edge of the square lattice is adjacent to two polygons (triangle or square) of opposite colors.

4.8.2 Slice transfer matrix

Any given 6V boundary is decomposed into vertical slices of unit width, made of a vertical sequence of $r - 1$ vertices. To each such slice we associate an $(r + 1) \times (r + 1)$ matrix T . The matrix T is defined recursively from the bottom to the top of the slice according to its 6V configurations as follows.

For illustration and help, we have represented in Fig.4.8 a typical slice configuration (a) in square/triangle decomposition and (b) in 6V form. We first consider the square/triangle decomposition of the 6V slice at hand, the vertices of which carry the initial data, say a_1, a_2, \dots, a_r from bottom to top on the left and b_1, b_2, \dots, b_r on the right. We further split all the squares into pairs of triangles by drawing their second diagonal. Note that horizontal edges are adjacent to two triangles of opposite colors. By a slight abuse of

language, we call again *rhombi* such pairs of triangles. With this definition, we are left with two unpaired triangles with edges $a_r - b_r$ and $a_1 - b_1$ respectively. This is repaired by adding the missing triangle of the opposite color on both top and bottom of the slice, with a third vertex carrying the value $a_{r+1} = b_{r+1} = 1$ and $a_0 = b_0 = 1$. As they all carry the same value 1, it will be convenient to identify all the vertices of the bottom layer as well as all those of the top one.

We label the lines supporting the horizontal edges of the 6V and the two extra rows of vertices by $1, 2, \dots, r + 1$, from bottom to top. We denote by T_i the matrix corresponding to the partial slice extending from lines 1 to i .

We start by defining $T_1 = H_{1,2}(a_1, b_1, x)$ if the bottom triangle is white and $T_1 = V_{1,2}(1, a_1, b_1)$ if it is gray, where x is the top vertex value of the rhombus containing the bottom triangle. Let us consider the vertices i and $i + 1$, for $i = 1, 2, \dots, r - 1$. If the 6V vertical edge between line i and $i + 1$ points up (resp. down), then T_{i+1} is obtained by multiplying T_i by an operator $V_{i,i+1}$ (resp. $H_{i,i+1}$) of Eqs. (4.9-4.10). Moreover the order of multiplication is from the left (resp. right) if the diagonal of the square is the first, connecting the SW and NE corners (resp. second, connecting NW to SE corners). This gives:

$$\begin{array}{cccccc}
 \begin{array}{|c|} \hline \blacksquare \\ \hline \end{array} & \begin{array}{|c|} \hline \square \\ \hline \end{array} & \begin{array}{|c|} \hline \blacksquare \\ \hline \end{array} & \begin{array}{|c|} \hline \square \\ \hline \end{array} & \begin{array}{|c|} \hline \blacksquare \\ \hline \end{array} & \begin{array}{|c|} \hline \square \\ \hline \end{array} \\
 \begin{array}{c} \updownarrow \\ \leftarrow \rightarrow \end{array} & \begin{array}{c} \updownarrow \\ \leftarrow \rightarrow \end{array} \\
 \mathbf{T}_{i+1} = \mathbf{V}_{i,i+1} \mathbf{T}_i & \mathbf{H}_{i,i+1} \mathbf{T}_i & \mathbf{T}_i \mathbf{H}_{i,i+1} & \mathbf{T}_i \mathbf{V}_{i,i+1} & \mathbf{T}_i \mathbf{V}_{i,i+1} & \mathbf{T}_i \mathbf{H}_{i,i+1}
 \end{array} \tag{4.13}$$

The three arguments of the $V_{i,i+1}$ and $H_{i,i+1}$ operators are respectively (x_{i-1}, a_i, b_i) and (a_i, b_i, u_{i+1}) , where x_{i-1} (resp. u_{i+1}) is the third vertex label of the gray triangle with edge $a_i - b_i$. This defines $T = T_r$ uniquely.

Example 4.9. *Let us consider the case of Fig.4.8 (a)-(c). The total matrix $T = T_7$ is obtained recursively as follows:*

$$\begin{array}{l}
 T_1 = V_{1,2}(1, a_1, b_1) \quad T_2 = V_{2,3}(a_1, a_2, b_2) T_1 \quad T_3 = T_2 V_{3,4}(b_2, a_3, b_3) \quad T_4 = T_3 H_{4,5}(a_4, b_4, b_5) \\
 T_5 = H_{5,6}(a_5, b_5, b_6) T_4 \quad T_6 = T_5 V_{6,7}(b_6, a_7, b_7) \quad T_7 = H_{7,8}(a_7, b_7, 1) T_6
 \end{array}$$

4.8.3 Networks

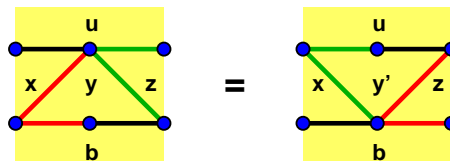
As pointed out earlier, the operators with respective indices $i, i + 1$ and $j, j + 1$ commute as soon as $j > i + 1$ or $j + 1 < i$. A useful way of representing the matrices $V_{i,i+1}$ and

$H_{i,i+1}$ is as networks. We start with the representation:

$$H_{i,i+1}(a, b, u) \qquad V_{i,i+1}(x, a, b) \qquad (4.14)$$

where the left vertices $i, i+1$ are connected to the right vertices $i, i+1$ via weighted edges $i \rightarrow j$ corresponding to the nonzero entries (i, j) of the matrices H, V of (4.4). More precisely, a diagonal entry 1 with indices (j, j) is coded by a thick black horizontal edge connecting the left vertex j to the right vertex j . The other nontrivial entries (j, k) are coded by thick green (resp. red) edges for H (resp. V), connecting the left vertex j to the right vertex k . The actual values of these nontrivial entries are coded by the labels of the faces of the network x, a, b, u in (4.14). Implicitly, the full representation of $H_{i,i+1}$ and $V_{i,i+1}$ as $r+1 \times r+1$ matrices also involves thick horizontal black edges connecting the left vertices $1, 2, \dots, i-1, i+2, \dots, r+1$ to their right counterparts, corresponding to the block form of (4.5), and which we omitted in (4.14) for simplicity.

The multiplication of two matrices is naturally coded by the concatenation of their networks, by identifying the right vertices of the network of the first matrix to the left ones of that of the second. The result is in general a rectangle of height $r+1$, and width possibly smaller than the number of matrices multiplied, as some horizontal black lines may be freely removed to gain space. We denote by $N(M)$ the network associated to the matrix M . For illustration, we have represented in Fig.4.8 (d) the network $N(T)$ corresponding to the matrix T of Example 4.9. As another example, the “mutation” Lemma 4.7 reads in network language:



The networks provide us with natural weighted path models. Indeed, the matrix entry $T_{m,p}$ is interpreted as the partition function for paths from left to right on the network of T , starting from the left vertex m and ending at the right vertex p , weighted by the product of weights of the edges visited, namely:

$$T_{m,p} = \sum_{\substack{\text{paths } m \rightarrow p \\ \text{on } N(T)}} \prod_{\substack{\text{edges } e \\ \text{visited}}} w(e) \qquad (4.15)$$

4.9 General solution as path model on networks

We now give the general expression for the solution $T_{\alpha,j,k}$ of the A_r T-system for arbitrary boundary conditions.

4.9.1 The case of $T_{1,j,k}$

As shown above, any boundary condition is coded by a configuration of the 6V model on an infinite strip of width $r - 1$ with the properties (i)-(ii) of Lemma 4.8.

Definition 4.10. *The projection of $(1, j, k)$ on the boundary is the portion of boundary between the broken lines ℓ_{j_0} and ℓ_{j_1} , containing the bottom vertices $(1, j_0, k_0)$ and $(1, j_1, k_1)$, respectively such that $j_0 - k_0 = j - k$ and $j_1 + k_1 = j + k$ with j_0 maximal and j_1 minimal.*

To this projection we naturally associate the corresponding truncated configuration \mathcal{C} of the 6V model on a rectangle of height $r - 1$ between the planes $j = j_0$ and $j = j_1$, and with face labels given by the original vertex values of the boundary. Let $\mathcal{T}_{j_0, j_1}(\mathcal{C})$ denote the product of vertical slice transfer matrices from the slice $(j_0, j_0 + 1)$ to the slice $(j_1 - 1, j_1)$. Then we have:

Theorem 4.11. *The solution of the A_r T-system with arbitrary fixed boundary reads for $\alpha = 1$:*

$$T_{1,j,k} = T_{1,j_1,k_1} (\mathcal{T}_{j_0,j_1}(\mathcal{C}))_{1,1} \quad (4.16)$$

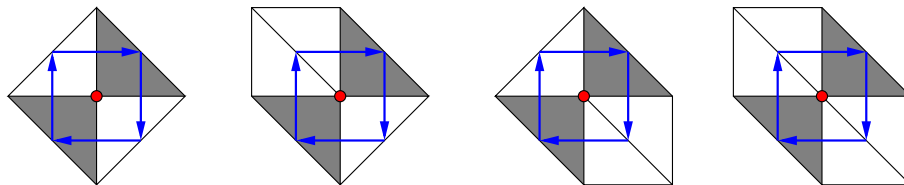
in the above notations.

Proof. This is proved by induction under mutation. First, (4.16) is satisfied for $\mathcal{C} = \mathcal{C}_0$, corresponding to the truncated basic staircase boundary. Indeed, we may rewrite (4.11) as

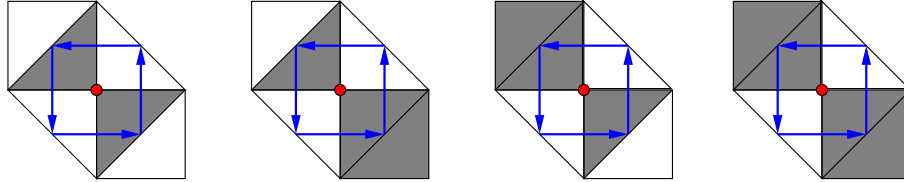
$$T_{1,j,k} = T_{1,j+k-1,1} \left(\prod_{i=0}^{k-2} B(\mathbf{a}(j - k + 1 + 2i), \mathbf{a}(j - k + 2 + 2i)) \times A(\mathbf{a}(j - k + 2 + 2i), \mathbf{a}(j - k + 3 + 2i)) \right)_{1,1}$$

by use of $A(\mathbf{a}, \mathbf{a}')_{1,j} = \delta_{j,1}$ and $B(\mathbf{a}, \mathbf{a}')_{j,1} = \delta_{j,1} a'_1 / a_1$. We see that this boils down to (4.16) with $k_0 = k_1 = 1$, $j_1 = j + k - 1$, and $j_0 = j - k + 1$. As explained above, any mutation μ may be implemented by an elementary loop reversal on the 6V configurations, and only mutations within the projection of $(1, j, k)$ affect the value of $T_{1,j,k}$.

Let us assume (4.16) holds for some 6V configuration with face labels \mathcal{C} . We wish to apply a mutation μ , i.e. form the configuration $\mu(\mathcal{C})$, identical to \mathcal{C} except for the reversed elementary loop and the updated face label. Assume this is a forward mutation, i.e. the corresponding loop is oriented clockwise in \mathcal{C} , and assume for definiteness that it occurs between vertical slices s and $s + 1$, with respective slice transfer matrices $T^{(s)}$ and $T^{(s+1)}$, and between horizontal lines i and $i + 1$. Due to the rules (4.13), examining the triangle decompositions of the four adjacent vertices to the loop, we find the following four possibilities:



Recalling that the choice of diagonal in the white squares is arbitrary, we may bring all situations to the first one, by use of the identity (4.10) within the relevant slice transfer matrices. Applying the mutation to this case amounts to the transformation of Fig.4.3 (b). We now have the following four possibilities for the environment of the reversed loop:



To recover the correct slice transfer matrices, we must flip the diagonals of the gray squares, by applying (4.9). Taking the product of transfer matrices over all slices, we finally get the “mutated” matrix $\mathcal{T}_{j_0, j_1}(\mu(\mathcal{C}))$. We may repeat the same argument for backward mutations, while exchanging the roles of white and gray triangles, and for mutations at vertices with $\alpha = 1$ and $\alpha = r$ with the obvious changes.

As before, we must however consider separately the case when the mutation occurs in the lower left or lower right square face of the truncated 6V configuration. In these cases indeed, the projection of $(1, j, k)$ is modified and we must drop (resp. insert) a first or last slice transfer matrix when the mutation is forward (resp. backward). As before, dropping/inserting a last slice transfer matrix implements the correct change of prefactor T_{1, j_1, k_1} that makes it agree with the new projection. In all cases, (4.16) follows for $\mu(\mathcal{C})$. This completes the proof of the Theorem. \square

4.9.2 Non-intersecting paths on networks and the case of $T_{\alpha, j, k}$

Let $N_{j_0, j_1}(\mathcal{C})$ denote the network associated to the transfer matrix $\mathcal{T}_{j_0, j_1}(\mathcal{C})$. We may interpret $T_{1, j, k}/T_{1, j_1, k_1}$ as the partition function for weighted paths on the network $N_{j_0, j_1}(\mathcal{C})$, that start at the left vertex 1 and end at the right vertex 1, namely:

$$\frac{T_{1, j, k}}{T_{1, j_1, k_1}} = \sum_{\substack{\text{paths } p: 1 \rightarrow 1 \\ \text{on } N_{j_0, j_1}(\mathcal{C})}} \prod_{\substack{\text{edges } e \\ \text{visited}}} w(e) \quad (4.17)$$

where $w(e)$ stands for the weight of the edge e .

Note that in the case of the basic staircase \mathcal{C}_0 , this path interpretation is different from that of Ref. [7]. Nevertheless, we may like in Ref. [7] interpret the determinant identity (4.2) that relates $T_{\alpha, j, k}$ to $T_{1, j, k}$ in terms of non-intersecting paths, now on networks.

Let us pick an arbitrary boundary \mathcal{C} , and rewrite the determinant formula (4.2) as:

$$\frac{T_{\alpha, j, k}}{\prod_{1 \leq b \leq \alpha} T_{1, j_1(b), k_1(b)}} = \det_{1 \leq a, b \leq \alpha} \left(\frac{T_{1, j-a+b, k+a+b-\alpha-1}}{T_{1, j_1(b), k_1(b)}} \right) \quad (4.18)$$

where we denote by $(1, j_1(b), k_1(b))$ the common rightmost bottom vertex of the projections onto the boundary \mathcal{C} of the vertices $(1, j - a + b, k + a + b - \alpha - 1)$, $a = 1, 2, \dots, \alpha$.

Similarly let us denote by $(1, j_0(a), k_0(a))$ the common leftmost bottom vertex of the projections onto the boundary \mathcal{C} of the vertices $(1, j - a + b, k + a + b - \alpha - 1)$, $b = 1, 2, \dots, \alpha$.

We denote by (j, x) the vertex of $N(\mathcal{C})$ that lies between the slices $j - 1, j$ and $j, j + 1$ at height x , namely the common exit and entry point x of respectively the network for the slice $j - 1, j$ and that for $j, j + 1$. For instance the left vertex x of $N_{a,b}(\mathcal{C})$ has coordinates (a, x) , while the right vertex of same height has coordinates (b, x) .

We finally have:

Theorem 4.12. *The solution $T_{\alpha,j,k}$ of the A_r T -system for arbitrary boundary is equal to $\prod_{1 \leq b \leq \alpha} T_{1,j_1(b),k_1(b)}$ times the partition function for families of α non-intersecting paths on the network $N(\mathcal{C})$, starting at the vertices $(j_0(a), 1)$, $a = 1, 2, \dots, \alpha$ and ending at the vertices $(j_1(b), 1)$, $b = 1, 2, \dots, \alpha$.*

Proof. In view of (4.16) and its reformulation in terms of paths on networks (4.17), we may interpret the (a, b) term in the determinant (4.18) as the partition function for paths from the bottom left to the bottom right vertex on the network $N_{j_0(a),j_1(b)}(\mathcal{C})$. The Theorem follows from the application of the Lindström-Gessel-Viennot theorem [17] [13]. \square

Corollary 4.13. *The solution $T_{\alpha,j,k}$ of the A_r T -system for arbitrary boundary condition $T_{\alpha,j,k_{\alpha,j}} = a_{\alpha,j}$ ($\alpha \in I_r, j \in \mathbb{Z}$) is a positive Laurent polynomial of its initial data $(a_{\alpha,j})_{\alpha \in I_r; j \in \mathbb{Z}}$.*

4.10 An example

Let us consider the case $r = 3$ and the boundary depicted in Fig.4.9, with the A_3 boundary condition that $T_{0,j,k} = T_{4,j,k} = 1$ for all j, k . We wish to compute $T_{2,3,3}$ in terms of the indicated boundary values (blue vertices):

$$\begin{aligned} T_{1,0,1} = a_1 \quad T_{1,1,0} = b_1 \quad T_{1,2,1} = c_1 \quad T_{1,3,2} = d_1 \quad T_{1,4,1} = e_1 \quad T_{1,5,0} = f_1 \quad T_{1,6,1} = g_1 \\ T_{2,0,0} = a_2 \quad T_{2,1,1} = b_2 \quad T_{2,2,2} = c_2 \quad T_{2,3,1} = d_2 \quad T_{2,4,0} = e_2 \quad T_{2,5,1} = f_2 \quad T_{2,6,2} = g_2 \\ T_{3,0,1} = a_3 \quad T_{3,1,0} = b_3 \quad T_{3,2,1} = c_3 \quad T_{3,3,0} = d_3 \quad T_{3,4,1} = e_3 \quad T_{3,5,0} = f_3 \quad T_{3,6,1} = g_3 \end{aligned}$$

We have the determinant formula

$$T_{2,3,3} = \begin{vmatrix} T_{1,3,2} & T_{1,4,3} \\ T_{1,2,3} & T_{1,3,4} \end{vmatrix} = \begin{vmatrix} T_{Q_1} & T_{Q_2} \\ T_{Q_3} & T_{Q_4} \end{vmatrix} \quad (4.19)$$

which involves the 4 points Q_1, Q_2, Q_3, Q_4 of the $\alpha = 1$ plane. In turn, the projections of the Q_i onto the boundary read: $X = (1, j_0(2), k_0(2)) = (1, 0, 1)$, $Y = (1, j_0(1), k_0(1)) = (1, j_1(1), k_1(1)) = (1, 3, 2)$ and $Z = (1, j_1(2), k_1(2)) = (1, 6, 1)$.

Next, we construct the 6V configuration with face labels of Fig.4.10 (a) corresponding to the boundary. The simplest way is to start from the basic staircase and apply to it the 3 mutations that bring it to the boundary under consideration (see the dashed lines in Fig.4.9 (b)). We also construct the triangle decomposition of Fig.4.10 (b), by drawing the diagonal reflection symmetry axes of the vertices and a second diagonal in

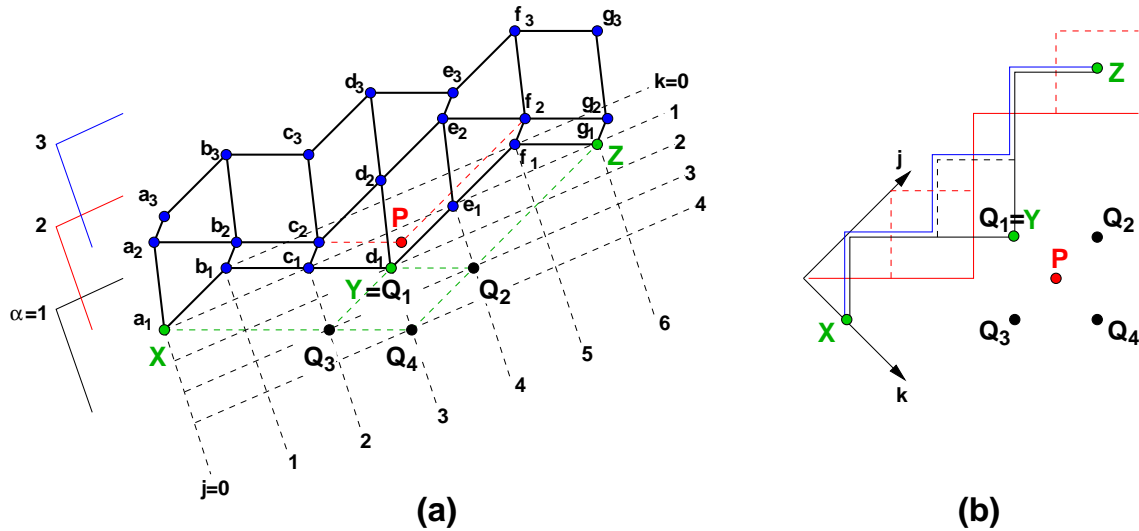


Figure 4.9: A view in perspective of a particular boundary (a) for the A_3 T-system (blue vertices and thick solid black edges). We have indicated the three horizontal layers $\alpha = 1, 2, 3$, and the j, k coordinates at $\alpha = 1$. We have represented the vertex $P = (2, 3, 3)$ and the four points of the $\alpha = 1$ layer $Q_1 = (1, 3, 2), Q_2 = (1, 4, 3), Q_3 = (1, 2, 3), Q_4 = (1, 3, 4)$ involved in the determinant formula (4.19). The projections of the latter onto the boundary are $X = (1, 0, 1), Y = Q_1 = (1, 3, 2)$ and $Z = (1, 6, 1)$. We also represent the same information (b) in projection onto the (k, j) plane, with layers $\alpha = 1, 2, 3$ represented respectively in black, red, blue. We have also indicated in dashed lines the mutations leading to this boundary from the basic staircase one.

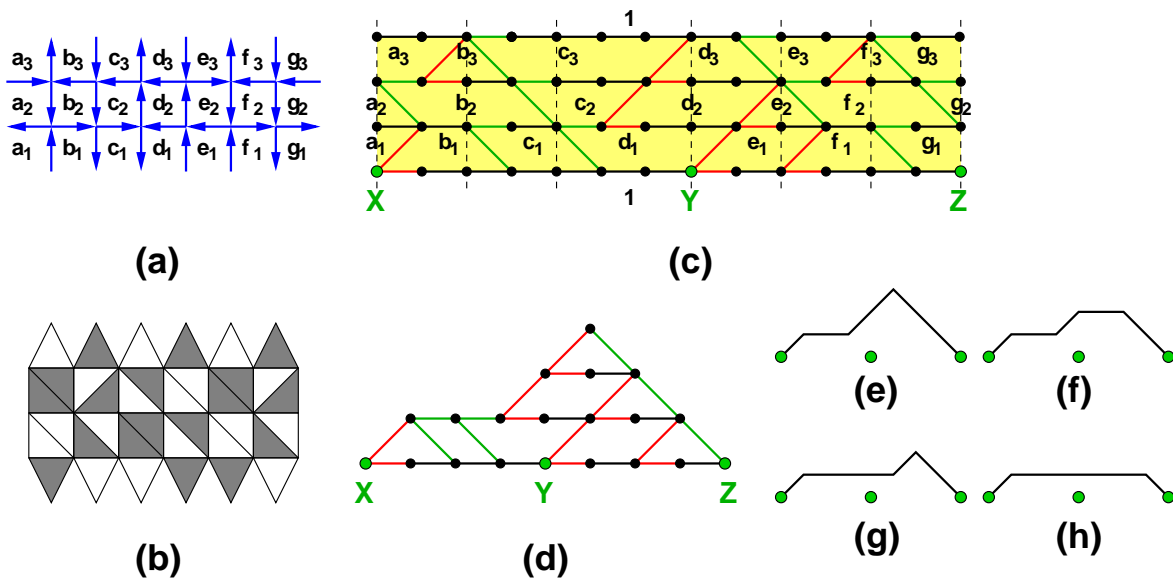


Figure 4.10: The $6V$ version of the boundary of Fig.4.9 (a) with its face labels and the corresponding triangle decomposition of the dual (b). The associated network (c) is represented with an indication of the successive slices (vertical dashed lines) and the corresponding face labels. The truncation (d) of the network is the only information needed to get the result. The partition function for paths from X to Z that do not visit Y is a weighted sum over the four paths (e),(f),(g),(h).

the remaining squares. This allows to build the network of Fig.4.10 (c), by following the above procedure. In particular the edge-weights of the network are given by the surrounding face labels according to the rules (4.14).

The Lindström-Gessel-Viennot theorem expresses $T_{2,3,3}/(T_{1,3,2}T_{1,6,1})$ as the partition function for pairs of non-intersecting paths on this network that start at X, Y and end at Y, Z . This is simply the partition function for a single path from X to Z that does not visit Y . To compute the latter, we may restrict ourselves to the truncation of the network depicted in Fig.4.10 (d), where the edges keep their original weights from (c). The partition function is therefore a weighted sum over the four paths (e),(f),(g),(h), and the final formula follows:

$$\frac{T_{2,3,3}}{T_{1,3,2}T_{1,6,1}} = \frac{1}{d_3g_1} + \frac{c_3d_3}{d_2d_3g_1} + \frac{c_2e_1e_3}{d_1d_2e_2g_1} + \frac{c_2f_2}{d_1e_2g_1} \quad (4.20)$$

5 Application: Q -system from the T -system solutions

In this section, we compare the restriction of our T -system solution to the case of the A_r Q -system whose solution was worked out in [5]. We find alternative path models for describing the general solutions.

5.1 Q system

The Q -system for A_r is obtained from the T -system by “forgetting” about the variable j . This can be done in various ways, here we adopt the following: we impose that the solution and the initial data be periodic, namely that $T_{\alpha, j+2, k} = T_{\alpha, j, k}$ for all α, j, k . In this case, the quantities $R_{\alpha, k} = T_{\alpha, \alpha+k [2], k}$ are easily seen to satisfy the A_r Q -system:

$$\begin{aligned} R_{\alpha, k+1}R_{\alpha, k-1} &= R_{\alpha, k}^2 + R_{\alpha+1, k}R_{\alpha-1, k} \\ R_{0, k} &= R_{r+1, k} = 1 \end{aligned} \quad (5.1)$$

In [5], the boundary data for (5.1) were shown to be in bijection with Motzkin paths of length $r-1$, $\mathbf{m} = (m_1, m_2, \dots, m_r)$, and to take the form $x_{\mathbf{m}} = \{R_{\alpha, m_\alpha}, R_{\alpha, m_{\alpha+1}}\}_{\alpha=1}^r$. The explicit solution $R_{\alpha, k}$ for each such data was expressed as follows. First, for each Motzkin path \mathbf{m} one constructs an explicit rooted oriented graph $\Gamma_{\mathbf{m}}$ with $2r+2$ vertices, and with weighted edges encoded in a $2r+2 \times 2r+2$ transfer matrix $T_{\mathbf{m}}$. The root corresponds to the row and column index 1 of the transfer matrix. The matrix $T_{\mathbf{m}}$ is constructed in such a way that any oriented edge $i \rightarrow j$ of $\Gamma_{\mathbf{m}}$ going away from the root (“ascent”) has a trivial weight 1, while any oriented edge $i \rightarrow j$ pointing toward the root (“descent”) has some-non-trivial weight $t \times y_{i, j}(\mathbf{m})$, the latter being a Laurent monomial of the initial data. The main result of [5] for $\alpha = 1$ reads:

$$R_{1, n+m_1} = R_{1, m_1} \left((I - T_{\mathbf{m}})^{-1} \right)_{1,1} \Big|_{t^n} \quad (5.2)$$

where the notation $X|_{t^n}$ denotes the coefficient of t^n in X . In other words, the quantity $R_{1, n+m_1}/R_{1, m_1}$ is the partition function for paths from and to the root on $\Gamma_{\mathbf{m}}$, with exactly n descents.

Example 5.1. For the case of A_3 , the transfer matrix $T_{2,1,0}$ for the Motzkin path $(2, 1, 0)$ reads [5]:

$$T_{2,1,0} = \begin{pmatrix} 0 & 1 & 0 & 0 & 0 & 0 & 0 & 0 \\ ty_1 & 0 & 1 & 0 & 0 & 0 & 0 & 0 \\ 0 & ty_2 & 0 & 1 & 1 & 0 & 0 & 0 \\ 0 & 0 & ty_3 & 0 & 0 & 0 & 0 & 0 \\ 0 & ty_{3,1} & ty_4 & 0 & 0 & 1 & 1 & 0 \\ 0 & 0 & 0 & 0 & ty_5 & 0 & 0 & 0 \\ 0 & ty_{4,1} & ty_{4,2} & 0 & ty_6 & 0 & 0 & 1 \\ 0 & 0 & 0 & 0 & 0 & 0 & ty_7 & 0 \end{pmatrix} \quad (5.3)$$

where:

$$y_1 = \frac{R_{1,3}}{R_{1,2}}, y_2 = \frac{R_{2,2}^2}{R_{2,1}R_{1,2}R_{1,3}}, y_3 = \frac{R_{1,2}R_{2,2}}{R_{2,1}R_{1,3}}, y_4 = \frac{R_{1,2}^2R_{3,1}^2}{R_{3,0}R_{2,1}R_{2,2}R_{1,3}}, y_5 = \frac{R_{2,1}R_{3,1}}{R_{3,0}R_{2,2}} \\ y_6 = \frac{R_{2,1}^2}{R_{3,0}R_{3,1}R_{2,2}}, y_7 = \frac{R_{3,0}}{R_{3,1}}, y_{4,2} = \frac{R_{1,2}^2}{R_{3,0}R_{2,2}R_{1,3}}, y_{3,1} = \frac{R_{3,1}^2}{R_{3,0}R_{2,1}R_{1,3}}, y_{4,1} = \frac{1}{R_{3,0}R_{1,3}} \quad (5.4)$$

The general solution for $R_{\alpha,n}$ was shown in [5] to be expressible as partition function for families of α strongly non-intersecting weighted paths on $\Gamma_{\mathbf{m}}$, via a generalization of the Lindström-Gessel-Viennot Theorem.

5.2 Network formulation from T -system

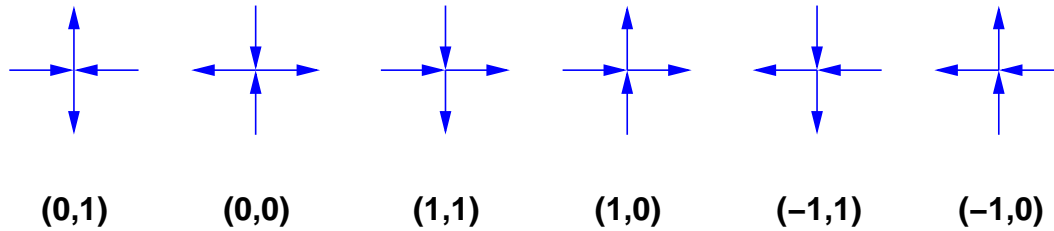
As mentioned above, the Q -system restriction amounts to having a periodic solution of the T -system, with period 2 in the variable j . For such a solution, boundaries are much simpler, as they are also 2-periodic in the j direction. However, constructing such a boundary by iterated mutations on the basic staircase (which has the desired periodicity) involves repeating each mutation an infinite number of times (with periodicity 2 in the j direction). So *stricto sensu* these boundaries are not covered by our previous solution. But for each fixed value of (α, j, k) only a finite portion of the boundary is needed to express $T_{\alpha,j,k}$. So we may apply a finite number of mutations for each case and get the correct result, and just formally complete the boundary by periodicity. We may therefore apply the results of Section 4 here.

In the periodic case, the boundary values must read $T_{\alpha,0,k_{\alpha,0}}$ and $T_{\alpha,1,k_{\alpha,1}}$ for $j = 0, 1 \pmod 2$ respectively. Note that $k_{\alpha,1} - k_{\alpha,0} = \pm 1$. Defining $m_\alpha = \text{Min}(k_{\alpha,0}, k_{\alpha,1})$, $m_\alpha + 1 = \text{Max}(k_{\alpha,0}, k_{\alpha,1})$, we find that \mathbf{m} is the relevant Motzkin path for describing the Q -system boundary data.

According to our results, each periodic boundary may be viewed as a configuration of the 6V model but now with a periodicity of 2 in the direction of the strip. In other words, we have a configuration of the 6V model on a cylinder of perimeter 2 and height $r - 1$. Moreover, as we started from a configuration with alternating vertical arrows (spin 0 with two edges) on both the bottom and the top of the strip, any mutated configuration has one vertical edge pointing up and one pointing down on the upper and lower boundaries of the cylinder. We have the following:

Lemma 5.2. *The 6V configurations on a cylinder of perimeter 2 and height $r - 1$ with alternating edge orientations on top and bottom are in bijection with Motzkin paths of length $r - 1$, with $m_1 = 0$ or 1.*

Proof. The bijection goes as follows. We start from a Motzkin path $\mathbf{m} = (m_1, m_2, \dots, m_r)$, with $m_1 = 0$ or 1. Then we have three possible situations for each of the $r - 1$ steps of the Motzkin path: $x_i = m_{i+1} - m_i = 0, -1$, or 1, and two possible values for $y_i = i + m_i = 0, 1$ modulo 2, for $i = 1, 2, \dots, r - 1$. We have the following dictionary between the six possible pairs (x_i, y_i) and the six vertices of the 6V model.



More simply, x_i is the “algebraic sum” of the two horizontal edges (0 if they are opposed, 1 if they both point to the right, -1 if they both point to the left) and y_i is determined only by the bottom vertical edge (1 if it points down, 0 if it points up).

Let us arrange the vertices associated to $\{(x_i, y_i)\}_{i=1}^{r-1}$ on a single column, from bottom to top. Note that the rules above make the orientations of edges compatible, so we can identify the bottom vertical edge of the vertex $i + 1$ with the top vertical edge of the vertex i . There is a unique way to complete this configuration into one on the $2 \times r - 1$ cylinder. We must indeed add a second column of vertices which are identical to the previous ones, up to reversal of all vertical arrows (the unique solution respecting the ice rule), in order to satisfy both the horizontal periodic boundary condition and the alternating one on top and bottom. Note that $m_1 = 0$ or 1 determines whether the bottom left vertical edge points down or up. \square

Example 5.3. *We consider the case $r = 3$ and the Motzkin path $(2, 1, 0)$. We have $x_i = -1, y_i = 1$ for $i = 1, 2$. The 6V configuration is represented in Fig.5.1 (a). We have indicated the values of $k_{\alpha,j}$ in the faces of the configuration, corresponding to $\alpha = 1, 2, 3$ and $j = 0, 1$. These are not to be mistaken for the usual face labels of the 6V configuration, which are the assigned boundary data $a_{\alpha,j}$ for the corresponding vertices: $T_{\alpha,j,k_{\alpha,j}} = a_{\alpha,j}$.*

To each Motzkin path $\mathbf{m} = (m_1, m_2, \dots, m_r)$, we may now associate a configuration of the 6V model on a cylinder of perimeter 2 and height $r - 1$ via Lemma 5.2 by using the shifted Motzkin path $\mathbf{m}' = \mathbf{m} - 2(p, p, \dots, p)$, where $p = \lfloor \frac{m_1}{2} \rfloor$. The corresponding values of $k_{\alpha,j}$ are uniquely determined by the Ampère rule and by $m_\alpha = \text{Min}(k_{\alpha,0}, k_{\alpha,1})$, $m_\alpha + 1 = \text{Max}(k_{\alpha,0}, k_{\alpha,1})$. The solutions for $T_{1,j,k}$ of Theorem 4.11 and for $T_{\alpha,j,k}$ of Theorem 4.12 involve only two types of slice transfer matrices, due to the periodicity, namely that for all slices of the form $[2a, 2a + 1]$ and that for $[2a - 1, 2a]$. These are coded by the two columns of the 6V configuration, which have the same horizontal edge orientations and

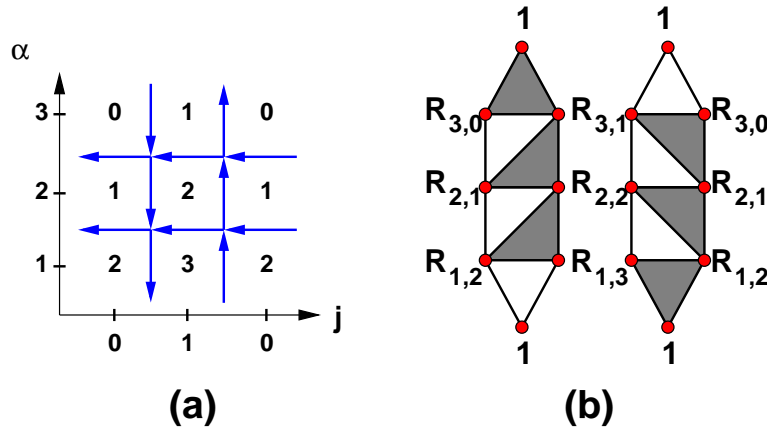


Figure 5.1: The periodic 6V configuration (a) associated to the Motzkin path $(2, 1, 0)$ for $r = 3$. The corresponding boundary vertices (α, j, k) may be read off the configuration: the third index k is determined by the Ampère rule and by $m_1 = 2$, and is indicated in each face. We have also sketched the associated rhombus/triangle decomposition (b) of the two corresponding slices, with the assigned boundary values.

opposite vertical ones. Using the construction of Sect. 4.8.2, the slice transfer matrices may be constructed inductively as follows, directly from the Motzkin path \mathbf{m} :

We start from m_1 . If it is even, the first slice transfer matrix has $T_1 = H_{1,2}$, if it is odd it has $T_1 = V_{1,2}$. Then, having constructed T_i , say with a last factor $H_{i,i+1}$ (resp. $V_{i,i+1}$), we have three possibilities (according to the value of $x_i = m_{i+1} - m_i$):

- (i) $x_i = 0$: then $T_{i+1} = V_{i,i+1}T_i = T_iV_{i,i+1}$ (resp. $T_{i+1} = H_{i,i+1}T_i = T_iH_{i,i+1}$).
- (ii) $x_i = 1$: then $T_{i+1} = T_iH_{i,i+1}$ (resp. $T_{i+1} = V_{i,i+1}T_i$).
- (iii) $x_i = -1$: then $T_{i+1} = H_{i,i+1}T_i$ (resp. $T_{i+1} = T_iV_{i,i+1}$).

The arguments of the matrices are, as usual, the boundary data at the vertices of the gray triangles, with the vertex indices of the form $(\alpha, j, k_{\alpha,j})$ where $k_{\alpha,j}$ are determined by \mathbf{m} . This gives a matrix $U_{\mathbf{m}} = T_r$ for each Motzkin path \mathbf{m} . The second slice is treated analogously. Due to the fact that its 6V configuration is identical to the first up to reversal of all vertical arrow, it is easy to write the corresponding slice transfer matrix $\tilde{U}_{\mathbf{m}}$ in terms of $U_{\mathbf{m}}$. Indeed, the rhombus/triangle decomposition of the second slice is the reflection of the first w.r.t. a vertical axis, and with all colors of triangles inverted. We therefore have to interchange $H \leftrightarrow V$, and to reverse the order of the factors. More precisely, let $*$ be the involutive anti-automorphism $((ab)^* = b^*a^*, (a^*)^* = a)$ such that $V_{i,i+1}^* = H_{i,i+1}$, then we have $\tilde{U}_{\mathbf{m}} = (U_{\mathbf{m}})^*$.

Example 5.4. *In the case of the Motzkin path $(2, 1, 0)$ for $r = 3$, we easily read the*

transfer matrices on the rhombus/triangle decomposition of Fig.5.1 (b):

$$\begin{aligned}
U_{2,1,0} &= H_{3,4}(R_{3,0}, R_{3,1}, 1)H_{2,3}(R_{2,1}, R_{2,2}, R_{3,1})H_{1,2}(R_{1,2}, R_{1,3}, R_{2,2}) \\
&= \begin{pmatrix} 1 & 0 & 0 & 0 \\ \frac{R_{2,2}}{R_{1,3}} & \frac{R_{1,2}}{R_{1,3}} & 0 & 0 \\ \frac{R_{3,1}}{R_{1,3}} & \frac{R_{1,2}R_{3,1}}{R_{1,3}R_{2,2}} & \frac{R_{2,1}}{R_{2,2}} & 0 \\ \frac{1}{R_{1,3}} & \frac{R_{1,2}}{R_{1,3}R_{2,2}} & \frac{R_{2,1}}{R_{2,2}R_{3,1}} & \frac{R_{3,0}}{R_{3,1}} \end{pmatrix} \\
\tilde{U}_{2,1,0} &= V_{1,2}(1, R_{1,3}, R_{1,2})V_{2,3}(R_{1,2}, R_{2,2}, R_{2,1})V_{3,4}(R_{2,1}, R_{3,1}, R_{3,0}) \\
&= \begin{pmatrix} \frac{R_{1,3}}{R_{1,2}} & \frac{R_{2,2}}{R_{1,2}R_{2,1}} & \frac{R_{3,1}}{R_{2,1}R_{3,0}} & \frac{1}{R_{3,0}} \\ 0 & \frac{R_{2,2}}{R_{2,1}} & \frac{R_{1,2}R_{3,1}}{R_{2,1}R_{3,0}} & \frac{R_{1,2}}{R_{3,0}} \\ 0 & 0 & \frac{R_{3,1}}{R_{3,0}} & \frac{R_{2,1}}{R_{3,0}} \\ 0 & 0 & 0 & 1 \end{pmatrix} \tag{5.5}
\end{aligned}$$

Let us apply the result of Theorem 4.11, with $k_0 = m_1 + 1 = k_1$ and $k = n + m_1$, $j_0 = j - n + 1$, $j_1 = j + n - 1$. Defining $\epsilon = 1 - (k \bmod 2)$ and $\theta = j_1 \bmod 2$, we get:

$$\begin{aligned}
R_{1,n+m_1} &= T_{1,\epsilon,k} = T_{1,\theta,k_1} \left((\tilde{U}_{\mathbf{m}} U_{\mathbf{m}})^{n-1} \right)_{1,1} \\
&= R_{1,m_1+1} \left((\tilde{U}_{\mathbf{m}} U_{\mathbf{m}})^{n-1} \right)_{1,1} = R_{1,m_1} \left((U_{\mathbf{m}} \tilde{U}_{\mathbf{m}})^n \right)_{1,1}
\end{aligned}$$

by use of $(U_{\mathbf{m}})_{1,x} = \delta_{1,x}$ and $(\tilde{U}_{\mathbf{m}})_{x,1} = \delta_{x,1} T_{1,1-\theta,k_1-1} / T_{1,\theta,k_1} = \delta_{x,1} R_{1,m_1} / R_{1,m_1+1}$. Comparing this with (5.2), we deduce the

Theorem 5.5. *Let \mathbf{m} be a Motzkin path of length $r - 1$, $T_{\mathbf{m}}$ the $2r + 2 \times 2r + 2$ transfer matrix of the Q -system solution of Ref. [5], and $U_{\mathbf{m}}$, $\tilde{U}_{\mathbf{m}}$ as above. Then we have an identity between “resolvents”:*

$$\left((I - T_{\mathbf{m}})^{-1} \right)_{1,1} = \left((I - tU_{\mathbf{m}}\tilde{U}_{\mathbf{m}})^{-1} \right)_{1,1}$$

Note that the matrices $U_{\mathbf{m}}$ and $\tilde{U}_{\mathbf{m}}$ have size $r + 1 \times r + 1$. We may however view the product $U_{\mathbf{m}}\tilde{U}_{\mathbf{m}}$ as the transfer matrix of a weighted graph $G_{\mathbf{m}}$ with $2r + 2$ vertices labeled $1, 2, \dots, (r + 1), 1', 2', \dots, (r + 1)'$, defined as follows. We interpret the matrix element $(U_{\mathbf{m}})_{i,j}$ as coding the weights of the oriented edge $i \rightarrow j'$ of $G_{\mathbf{m}}$ while $(\tilde{U}_{\mathbf{m}})_{i,j}$ codes the weight of the oriented edge $i' \rightarrow j$. Alternatively, we may form the 2×2 block transfer matrix $\theta_{\mathbf{m}} = \begin{pmatrix} 0 & \tilde{U}_{\mathbf{m}} \\ U_{\mathbf{m}} & 0 \end{pmatrix}$ for $G_{\mathbf{m}}$ and note that $\left((I - \sqrt{t}\theta_{\mathbf{m}})^{-1} \right)_{1,1} = \left((I - tU_{\mathbf{m}}\tilde{U}_{\mathbf{m}})^{-1} \right)_{1,1}$.

Noting that the non-zero elements of $\tilde{U}_{\mathbf{m}}$ have the same indices as those of the transpose of $U_{\mathbf{m}}$, we see that $G_{\mathbf{m}}$ has doubly oriented edges only, with specific weights for each orientation. From the network construction, all these weights are Laurent monomials of the initial data.

Example 5.6. For the Motzkin path $\mathbf{m} = (2, 1, 0)$ of $r = 3$, we may use the matrices (5.5). Without altering the resolvent, we may gauge-transform the matrices $U_{\mathbf{m}}$ and $\tilde{U}_{\mathbf{m}}$ with invertible matrices R, L with $L_{j,1} = L_{1,j} = \delta_{j,1}$: $V_{\mathbf{m}} = L^{-1}U_{\mathbf{m}}R$ and $\tilde{V}_{\mathbf{m}} = R^{-1}\tilde{U}_{\mathbf{m}}L$. For the choices:

$$L = \text{diag}\left(1, \frac{R_{1,2}R_{2,1}}{R_{2,2}}, \frac{R_{2,1}R_{3,0}}{R_{3,1}}, R_{3,0}\right) \quad R = \text{diag}(1, R_{1,2}, R_{2,1}, R_{3,1})$$

we find that

$$V_{\mathbf{m}} = \begin{pmatrix} 1 & 0 & 0 & 0 \\ y_2 & y_3 & 0 & 0 \\ y_{3,1} & y_4 & y_5 & 0 \\ y_{4,1} & y_{4,2} & y_6 & 1 \end{pmatrix} \quad \tilde{V}_{\mathbf{m}} = \begin{pmatrix} y_1 & 1 & 1 & 1 \\ 0 & 1 & 1 & 1 \\ 0 & 0 & 1 & 1 \\ 0 & 0 & 0 & y_7 \end{pmatrix}$$

in terms of the parameters of (5.4). One checks directly the statement of Theorem 5.5 with the matrix (5.3) and by computing the rational fraction $\left((I - tV_{\mathbf{m}}\tilde{V}_{\mathbf{m}})^{-1}\right)_{1,1}$.

Finally, turning to $R_{\alpha,n}$ for $\alpha > 1$, we have a simpler picture than in [5], as the quantity $R_{\alpha,n+m_1}/(R_{\alpha,m_1})^\alpha$ is expressed directly as the partition function for α non-intersecting paths on the associated network, without having to generalize the Lindström-Gessel-Viennot Theorem.

6 Conclusion

In this paper we have presented an explicit solution of the A_r T -system in terms of arbitrary boundary data. This solution is expressed in terms of partition functions of weighted paths on some particular networks, determined by the boundary.

We have briefly described the connection of the T -system to a particular cluster algebra. In particular, the sets of boundary data we have considered here form only a subset of the clusters in this cluster algebra. What happens is that the form of the cluster mutations can change in general from the equation (1.1), in some sense, the equation itself evolves, leading to clusters of a different kind. Nevertheless, the positivity conjecture seems to hold for these other clusters as well. It would be extremely interesting to probe whether these other clusters also have a description in terms of networks, that would make the Laurent positivity property manifest, like in the cases studied in this paper.

Another possible direction of generalization concerns non-commutative cluster algebras. In [8], the cluster algebra for the non-commutative A_1 Q -system was introduced, and its positivity proved by use of a non-commutative weighted path model. We have checked that it can be reformulated as a non-commutative network model in the spirit of the present paper, but with transfer matrices with entries in a non-commutative algebra. We hope to report on this direction in a later publication.

After completion of this paper, we became aware of Ref.[3], which deals with similar problems, but from a different point of view.

Acknowledgments. We would like to thank R. Kedem for numerous discussions. We also thank S. Fomin for hospitality at the University of Michigan and many discussions while this work was completed. We received partial support from the ANR Grant GranMa, the ENIGMA research training network MRTN-CT-2004-5652, and the ESF program MISGAM.

References

- [1] I. Assem, C. Reutenauer, and D. Smith, *Frises*, arXiv:0906.2026 [math.RA].
- [2] V. Bazhanov and N. Reshetikhin, *Restricted solid-on-solid models connected with simply-laced algebras and conformal field theory*. J. Phys. A: Math. Gen. **23** (1990) 1477–1492.
- [3] F. Bergeron and C. Reutenauer, *SL_k -Tilings of the Plane*, arXiv:1002.1089 [math.CO].
- [4] P. Di Francesco and R. Kedem, *Q -systems as cluster algebras II*, Lett. Math. Phys. **89** (2009) 183–216, arXiv:0803.0362 [math.RT].
- [5] P. Di Francesco and R. Kedem, *Q -systems, heaps, paths and cluster positivity*, Comm. Math. Phys. **293** No. 3 (2009) 727–802, DOI 10.1007/s00220-009-0947-5. arXiv:0811.3027 [math.CO].
- [6] P. Di Francesco and R. Kedem, *Q -system cluster algebras, paths and total positivity*, SIGMA **6** (2010) 014, 36 pages, arXiv:0906.3421 [math.CO].
- [7] P. Di Francesco and R. Kedem, *Positivity of the T -system cluster algebra*, Elec. Jour. of Comb. Vol. **16(1)** (2009) R140, Oberwolfach preprint OWP 2009-21, arXiv:0908.3122 [math.CO].
- [8] P. Di Francesco and R. Kedem, *Discrete non-commutative integrability: proof of a conjecture by M. Kontsevich*, Int. Math. Res. Notices (2010), 10.1093/imrn/rnq024, arXiv:0909.0615 [math-ph].
- [9] C. Dodgson, *Condensation of determinants*, Proceedings of the Royal Soc. of London **15** (1866) 150–155.
- [10] S. Fomin And A. Zelevinsky *Total positivity: tests and parameterizations*, Math. Intelligencer **22** (2000), 23-33. arXiv:math/9912128 [math.RA].
- [11] S. Fomin and A. Zelevinsky *Cluster Algebras I*. J. Amer. Math. Soc. **15** (2002), no. 2, 497–529 arXiv:math/0104151 [math.RT].
- [12] E. Frenkel and N. Reshetikhin, *The q -characters of representations of quantum affine algebras and deformations of W -algebras*. In Recent developments in quantum affine algebras and related topics (Raleigh, NC 1998), Contemp. Math. **248** (1999), 163–205.
- [13] I. M. Gessel and X. Viennot, *Binomial determinants, paths and hook formulae*, Adv. Math. **58** (1985) 300-321.

- [14] A. Henriquès, *A periodicity theorem for the octahedron recurrence*, J. Algebraic Comb. **26** No1 (2007) 1-26. [arXiv:math/0604289](#) [math.CO].
- [15] A. Knutson, T. Tao, and C. Woodward, *A positive proof of the Littlewood-Richardson rule using the octahedron recurrence*, Electr. J. Combin. **11** (2004) RP 61. [arXiv:math/0306274](#) [math.CO]
- [16] A. Kuniba, A. Nakanishi and J. Suzuki, *Functional relations in solvable lattice models. I. Functional relations and representation theory*. International J. Modern Phys. A **9** no. 30, pp 5215–5266 (1994).
- [17] B. Lindström, *On the vector representations of induced matroids*, Bull. London Math. Soc. **5** (1973) 85-90.
- [18] H. Nakajima, *t-analogs of q-characters of Kirillov-Reshetikhin modules of quantum affine algebras*, Represent. Theory **7** (2003), 259–274 (electronic).
- [19] A. Postnikov, *Total positivity, Grassmannians, and networks*. [arXiv:math/0609764v1](#) [math.CO].
- [20] D. Robbins and H. Rumsey, *Determinants and Alternating Sign Matrices*, Advances in Math. **62** (1986) 169-184.
- [21] D. Speyer, *Perfect matchings and the octahedron recurrence*, J. Algebraic Comb. **25** No 3 (2007) 309-348. [arXiv:math/0402452](#) [math.CO].